arXiv:cond-mat/9610196v1 [cond-mat.stat-mech] 28 Oct 1996

Real-Space Renormalization Group Methods Applied to Quantum Lattice Hamiltonians

Miguel A. Martín-Delgado[1]

[1]*Departamento de Física Teórica I, Universidad Complutense. 28040-Madrid, Spain*

(October 96)

Abstract

I review recent work and some new results, performed in collaboration with G. Sierra, on the Real-Space Renormalization group method applied to quantum spin lattice systems mainly in spatial dimensions one and two, and to spin ladders which are somehow in between. The first part of these notes is devoted to non-interacting systems in 1D and 2D and the role played by the correlations between blocks. The second part comprises interacting systems in 1D, spin ladders and 2D using the standard BRG method.

Proceedings of the El Escorial Summer School 1996 on STRONGLY CORRELATED MAGNETIC AND SUPERCONDUCTING SYSTEMS

I. INTRODUCTION: BRIEF HISTORY OF REAL-SPACE RG METHODS

The Real-Space Renormalization Group Method has undergone a great revival since the Densty Matrix RG was introduce by White in 1992 [1], [2]. Nowdays, this method is considered a powerful numerical tool to get non-perturbative results, specially for interacting systems in 1D although some recent advances for 2D systems have been obtained [3], [2]. Despite being numerical, the DMRG has also been a source of inspiration for analytical

studies and this is the framework of the present notes. Moreover, much of the El Escorial Summer School has been devoted to real-space RG methods [2], [4], [5].

The Renormalization Group method has become one of the basic concepts in Physics, ranging from areas such as Quantum Field Theory and Statistical Mechanics to Condensed Matter Physics. The many interesting and relevant models encountered in these fields are usually not exactly solvable except for some privileged cases in one dimension. It is then when we resort to the RG method to retrieve the essential features of those systems in order to have a qualitative understanding of what the physics of the model is all about. This understanding is usually recasted in the form of a RG-flow diagram were the different possible behaviours of the model leap to the eyes.

Many authors in the past have contributed significantly to the idea of renormalization and it is out of the scope of these notes to give a detailed account on this issue.

We shall be dealing with the the version of the RG as introduced by Wilson [6] and Anderson [7] in their treatment of the Kondo problem, and subsequent developments of these ideas carried out by Drell et al. at the SLAC group [9] and Pfeuty et al. [10].

Real space Renormalization Group (RG) methods originated from the study of the Kondo problem by Wilson [6]. It was clear from the beginning that one could not hope to achieve the accuracy Wilson obtained for the Kondo problem when dealing with more complicated many-body quantum Hamiltonians. The key difference is that in the Kondo model there exists a *recursion relation* for Hamiltonians at each step of the RG-elimination of degrees of freedom. The existence of such recursion relation facilitates enormously the work, but as it happens it is specific of *impurity problems*.

From the numerical point of view, the Block Renormalization Group (BRG) procedure proved to be not fully reliable in the past particularly in comparison with other numerical approaches, such as the Quantum MonteCarlo method which were being developed at the same time. This was one of the reasons why the BRG methods remained undeveloped during the '80's until the begining of the '90's when they are making a comeback as one of the most powerful numerical tools when dealing with zero temperature properties of

many-body systems, a situation where the Quantum MonteCarlo methods happen to be particularly badly behaved as far as fermionic systems is concerned [8].

As it happens, the BRG gives a good qualitative picture of many properties exhibited by quantum lattice Hamiltonians: Fixed points, RG-flow, phases of the system etc. as well as good quantitative results for some properties such as ground state energy and others [9], [10], [11], [20]. However in some important instances the BRG method is off the correct values of critical exponents by a sensible amount.

The origin of the density matrix RG method relies on the special treatment carried out by White and Noack [17] on the 1D tight-binding model, the lattice version of a single particle in a box. It was Wilson [18] the first to point out the relevance of this simple model in understanding the sometimes bad numerical performance of the standard Block Renormalization Group (BRG) method. In reference [17] the authors proposed a method called Combination of Boundary Conditions (CBC) which performs extremely well as compared to the exact known solution of the model. Recently, we have studied the role played by the boundary conditions in the real-space renormalization group method [21] by constructing a new analytical BRG-method which is able to give the exact ground state of the model and the correct $1/N^2$-law for the energy of the first excited state in the large N(size)-limit.
Yet another branch of applications of DMRG inspired ideas is to use the Superblock formalism [17] without resorting to a Density Matrix. For instance, in [19] it has been found that the application of this formalism to the anisotropic Heisenberg model in 1D successfully improves the standard BRG results of Rabin [20].
The Density Matrix RG has been originally devised to deal with quantum lattice Hamiltonians. However, recent new applications have been developed by Nishino and coworkers [4], [24], [27] to address the renormalization of classical lattice models. One of the outcomes of these studies has been to state the relationship between Baxter's corner transfer matrix formalism and the Density Matrix RG of White (in 1D).

The number of new developments on this subject is constantly growing and it is not possible to give a full account of all of them here. More applications can be found in the

rest of contributions to these proceedings devoted to real-space RG methods.

II. REVIEW OF STANDARD BLOCK RENORMALIZATION GROUP METHODS (BRG)

For the sake of completeness and to set up the notation used throughout these notes, the block renormalization group method is revisited in this section along the lines of a new and unified reformulation of it based on the idea of the *intertwiner operator* T to be discussed below. This treatment is by all means equivalent to the standard approach presented by S.R. White in his contribution to this volume. This formulation has recently allowed us to introduce the new Variational and Fokker-Planck DMRG methods [12] on equal footing as the standard BRG method. For a more extensive account on this method we refer to [13] and chapter 11 of reference [14] and references therein.

Let us first summarize the main features of the real-space RG. The problem that one faces generically is that of diagonalizing a quantum lattice Hamiltonian H, i.e.,

$$H|\psi>= E|\psi> \tag{1}$$

where $|\psi>$ is a state in the Hilbert space $\mathcal{H}$. If the lattice has N sites and there are k possible states per site then the dimension of $\mathcal{H}$ is simply

$$dim\mathcal{H} = k^N \tag{2}$$

As a matter of illustration we cite the following examples: $k = 4$ (Hubbard model), $k = 3$ (t-J model), $k = 2$ (Heisenberg model) etc.

When N is large enough the eigenvalue problem (1) is out of the capability of any human or computer means unless the model turns out to be integrable which only happens in some instances in $d = 1$.

These facts open the door to a variety of approximate methods among which the RG-approach, specially when combined with other techniques (e.g. numerical, variational etc.),

is one of the most relevant. The main idea of the RG-method is the mode elimination or thinning of the degrees of freedom followed by an iteration which reduces the number of variables step by step until a more manageable situation is reached. These intuitive ideas give rise to a well defined mathematical description of the RG-approach to the low lying spectrum of quantum lattice hamiltonians.

To carry out the RG-program it will be useful to introduce the following objects:

- $\mathcal{H}$: Hilbert space of the original problem.
- $\mathcal{H}'$: Hilbert space of the effective degrees of freedom.
- H: Hamiltonian acting in $\mathcal{H}$.
- H': Hamiltonian acting in $\mathcal{H}'$ (effective Hamiltonian).
- T : embedding operator : $\mathcal{H}' \longrightarrow \mathcal{H}$
- $T^\dagger$:truncation operator : $\mathcal{H} \longrightarrow \mathcal{H}'$

The problem now is to relate H, H' and T. The criterium to accomplish this task is that H and H' have in common their low lying spectrum. An exact implementation of this is given by the following equation:

$$HT = TH' \tag{3}$$

which imply that if $\Psi'_{E'}$ is an eigenstate of H' then $T\Psi'_{E'}$ is an eigenstate of H with the same eigenvalue (unless it belongs to the kernel of T: $T\Psi'_{E'} = 0$), indeed,

$$HT\Psi'_{E'} = TH'\Psi'_{E'} = E'T\Psi'_{E'} \tag{4}$$

To avoid the possibility that $T\Psi' = 0$ with $\Psi' \neq 0$, we shall impose on T the condition,

$$T^\dagger T = 1_{\mathcal{H}'} \tag{5}$$

such that

$$\Psi = T\Psi' \Rightarrow \Psi' = T^{\dagger}\Psi \tag{6}$$

Condition (5) thus stablishes a one to one relation between $\mathcal{H}'$ and Im(T) in $\mathcal{H}$.
Observe that Eq. (3) is nothing but the commutativity of the following diagram:

$$\begin{array}{ccc} \mathcal{H}' & \xrightarrow{T} & \mathcal{H} \\ H' \downarrow & & \downarrow H \\ \mathcal{H}' & \xrightarrow{T} & \mathcal{H} \end{array}$$

Eqs. (3) and (5) characterize what may be called exact renormalization group method (ERG) in the sense that the whole spectrum of H' is mapped onto a part (usually the bottom part) of the spectrum of H. In practical cases though the exact solution of Eqs. (3) and (5) is not possible so that one has to resort to approximations (see later on). Considering Eqs. (3) and (5) we can set up the effective Hamiltonian H' as:

$$H' = T^{\dagger}HT \tag{7}$$

This equation does not imply that the eigenvectors of H' are mapped onto eigenvectors of H. Notice that Eq.(7) together with (5) does not imply Eq. (3). This happens because the converse of Eq.(5), namely $TT^{\dagger} \neq 1_{\mathcal{H}}$ is not true, since otherwise this equation together with (5) would imply that the Hilbert spaces $\mathcal{H}$ and $\mathcal{H}'$ are isomorphic while on the other hand the truncation inherent to the RG method assumes that $dim\mathcal{H}' < dim\mathcal{H}$.

What Eq.(7) really implies is that the mean energy of H' for the states Ψ' of $\mathcal{H}'$ coincides with the mean energy of H for those states of $\mathcal{H}$ obtained through the embedding T, namely,

$$< \Psi'|H'|\Psi' > = < T\Psi'|H|T\Psi' > \tag{8}$$

In other words $T\Psi'$ is used as a variational state for the eigenstates of the Hamiltonian H. In particular T should be chosen in such a way that the states truncated in $\mathcal{H}$, which go down to $\mathcal{H}'$, are the ones expected to contribute the most to the ground state of H. Thus Eq. (7) is the basis of the so called variational renormalization group method (VRG)

As a matter of fact, the VRG method was the first one to be proposed. The ERG came afterwards as a perturbative extension of the former (see later on).
More generally, any operator $\mathcal{O}$ acting in $\mathcal{H}$ can be "pushed down" or renormalized to a new operator $\mathcal{O}'$ which acts in $\mathcal{H}'$ defined by the formula,

$$\mathcal{O}' = T^{\dagger}\mathcal{O}T \tag{9}$$

Notice that Eq.(7) is a particular case of this equation if choose O to be the Hamiltonian H.

In so far we have not made use of the all important concept of the block, but a practical implementation of the VRG or ERG methods does require it. The central role played by this concept makes all the real-space RG-methods to be block methods.

Once we have established the main features of the RG-program, there is quite a freedom to implement specifically these fundamentals. We may classify this freedom in two aspects:

- The choice to how to reduce the size of the lattice.
- The choice of how many states to be retained in the truncation procedure.

We shall address the first aspect now. There are mainly two procedures to reduce the size of the lattice:

- by dividing the lattice into blocks with n_B sites each. This is the blocking method introduced by Kadanoff to treat spin lattice systems. See figure 1.
- by retrieving site by site of the lattice at each step of the RG-program. This is the procedure used by Wilson in his RG-treatment of the Kondo problem. This method is clearly more suitable when the lattice is one-dimensional.

We shall be dealing with the Kadanoff block methods mainly because they are well suited to perform analytical computations and because they are conceptually easy to be extended to higher dimensions. On the contrary, the DMRG method introduced by White [1] works

with the Wilsonian numerical RG-procedure what makes it intrinsically one-dimensional and difficult to be generalized to more dimensions. This situation has changed recently in part as S.R. White has devised a numerical improvement of the DMRG which is applicable to a 1/5-depleted 2D lattice [3]. We have formulated our Variational and Fokker-Planck DMRG procedures as block renormalization methods [12].

Block RG-methods have recently received also renewed attention in one-dimensional problems in connection to what is called a *quantum group* symmetry [15], [16]. Based upon this symmetry we have constructed a new BRG-method that we call q-RG which among other features it is able to predict the exact line of critical XXZ models in the Anisotropic Heisenberg model, unlike the standard BRG-method.

III. THE ROLE OF BOUNDARY CONDITIONS AND REAL-SPACE RG

The first advance in trying to understand the sometimes bad numerical performance of the BRG methods came in the understanding of the effect of *boundary conditions* (BC) on the standard RG procedure [17].

White and Noack [17] pointed out that the standard BRG approach of neglecting all connections to the neighbouring blocks during the diagonalization of the block Hamiltonian H_B introduces large errors which cannot be corrected by any reasonable increase in the number of states kept. Moreover, in order to isolate the origin of this problem they study an extremely simple model: a free particle in a 1D lattice. As a matter of fact, it was Wilson [18] who pointed out the importance of understanding real-space RG in the context of this simple tight-binding model where the standard BRG clearly fails as we are going to show.

The reason for this failure can be traced back to the importance of the boundary conditions in diagonalizing the states of a given block Hamiltonian H_B in which the lattice is decomposed into. Notice that in this fashion we are isolating a given block from the rest of the lattice and this applies a *particular BC* to the block. However, the block is not truly isolated! A statement which is the more relevant the more strongly correlated is the system under

consideration. Thus, if the rest of the lattice were there it would apply different BC's to the boundaries of the block. This in turn makes the standard block-diagonalization conceptually not faithfully suited to account for the interaction with the rest of the lattice.

Once the origin of the problem is brought about the solution is also apparent: devise a method to change the boundary conditions in the block in order to mimick the interaction with the rest of the lattice. This is called the Combination of Boundary Conditions (CBC) method which yields very good numerical results. This method has not yet been generalized to interacting systems. However in reference [1] an alternative approach is proposed under the name of Density Matrix Renormalization Group (DMRG) which applies to more general situations and also produces quite accurate results.

In a recent paper [21] we have reconsidered again the role of BC's in the real space RG method for the case of a single-particle problem in a box. The continuum version of this Hamiltonian is simply $H = -\frac{\partial^2}{\partial x^2}$. We shall consider open chains with two types of BC's at the ends:

$$\text{Fixed BC's:} \quad \psi(0) = \psi(L) = 0 \tag{10}$$

$$\text{Free BC's:} \quad \frac{\partial \psi}{\partial x}(0) = \frac{\partial \psi}{\partial x}(L) = 0 \tag{11}$$

The lattice version of H for each type of BC's is given as follows:

$$H_{Fixed} = \begin{pmatrix} 2 & -1 & & & & \\ -1 & 2 & -1 & & & \\ & -1 & 2 & & & \\ & & & \ddots & & \\ & & & & 2 & -1 \\ & & & & -1 & 2 \end{pmatrix}, \quad H_{Free} = \begin{pmatrix} 1 & -1 & & & & \\ -1 & 2 & -1 & & & \\ & -1 & 2 & & & \\ & & & \ddots & & \\ & & & & 2 & -1 \\ & & & & -1 & 1 \end{pmatrix} \tag{12}$$

The only difference between H_{Fixed} and H_{Free} appear at the first and last diagonal entry ($2 \leftrightarrow 1$). The exact solution of (12) is very well-known and we give it for completeness:

$$\text{Fixed BC's:} \quad \psi_n(j) = N_n^{Fx} \sin \frac{\pi(n+1)}{N+1} j, \quad E_n = 4 \sin^2(\frac{\pi(n+1)}{2(N+1)}) \tag{13}$$

$$\text{Free BC's:} \quad \psi_n(j) = N_n^{Fr} \cos \frac{\pi n}{N}(j - \frac{1}{2}), \quad E_n = 4 \sin^2(\frac{\pi n}{2N}) \tag{14}$$

$$j = 1, 2, \ldots, N; \qquad n = 0, 1, \ldots, N-1.$$

where the $N_n's$ are normalization constants and N is the number of sites of the chain.

Before getting into the problem of the renormalization of these Hamiltonians, it is worth to pointing out another physical realization of H_{Free}: *A simple magnon above a ferromagnetic background satisfies Free BC's.* See [21] for more details.

Now let us get to the problem of renormalizing the tight-binding Hamiltonians (12).

In figure 2 we show the ground state and first excited states of the chain with fixed and free BC's.

It is clear from Fig.2 that *a standard Block RG method is not appropiate to study the ground state of fixed BC's since this state is non-homogeneous while the block truncation does not take into account this fact.*

Each piece of the ground state within each block satisfies BC's which vary from block to block. This is the motivation of reference [17] to consider different BC's in the block method, yielding quite accurate results.

We observe that the standard RG method performs rather poorly as compared to the CBC method which yields quite the exact results.

The other alternative to the CBC method is the Density Matrix RG method which can be phrased by saying that the rest of the chain produces on every block the appropiate BC's to be applied to its ends, and it has the virtue that can be generalized to other models, something which is not the case as for the CBC method.

On the other hand, the ground state of H_{Free} is an homogeneous state (see Fig.2) which in turn suggests that a standard RG analysis may work for this type of BC's. We shall show that this is indeed the case if the RG procedure is properly defined. The key of our

RG-prescription is to notice that H_{Free} has a geometrical meaning: *H_{Free} is the incidence matrix of a graph*, and it is called minus the discrete laplacian $-\Delta$ of that graph. Notice that H_{Fixed} has not such geometrical interpretation, in fact, it concides with the Dynkin diagram of the algebra A_N.

Based on this observation the Kadanoff blocking is nothing but the breaking of the graph into N/n_s disconnected graphs of n_s sites each. We shall choose $n_s = 3$ in our later computation.

The previous geometrical interpretation of H_{Free} suggests that we choose the block Hamiltonian H_B to be the incidence matrix of a disconnected graph, namely,

$$H_B = \begin{pmatrix} 1 & -1 & & & & & \\ -1 & 2 & -1 & & & & \\ & -1 & 1 & & & & \\ & & & 1 & -1 & & \\ & & & -1 & 2 & -1 & \\ & & & & -1 & 1 & \\ & & & & & & \ddots \end{pmatrix}, \quad H_{BB} = \begin{pmatrix} 0 & & & & & & \\ & 0 & & & & & \\ & & 1 & -1 & & & \\ & & -1 & 1 & & & \\ & & & & 0 & & \\ & & & & & 1 & -1 \\ & & & & & -1 & 1 \\ & & & & & & \ddots \end{pmatrix} \tag{15}$$

andthe interblock Hamiltonian H_{BB} above describes the interaction between blocks.

H_{BB} in turn also coincides with the incidence matrix of a graph which contains the missing links which connects consecutive blocks. In a few words: our RG-prescription introduces free BC's at the ends of every block. This condition fixes uniquely the breaking of H_{Free} into the sum $H_B + H_{BB}$. This is the choice we make. It should be emphasized that the splitting of H_{Free} into two parts $H_B + H_{BB}$ is by no means unique, so that different choices may lead to very different results.

Prior to any computation we notice that the previous RG-prescription should lead to an exact value of the ground state energy, for the ground state of each block is again a constant function. The question is therefore to what extent our method is capable of describing the excited states. We shall concentrate ourselves to the first excited state since computations can be carried out analytically.

First of all we diagonalize H_B within each block of 3 sites, keeping only the ground state $\psi_0^{(0)}$ and the first excited state $\psi_1^{(0)}$ ($3 \to 2$ truncation). The superscript denotes the initial step in the truncation method. In figure 3 we picture the 3 eigenvectors for the 3-site Hamiltonian which will be the building blocks for our BRG, namely the two lowest ones. In the standard RG method we would choose $\psi_0^{(0)}$ and $\psi_1^{(0)}$ as the orthonormal basis for the truncated Hilbert space and obtain the effective Hamiltonian H'_B and H'_{BB}. In our case it is convenient to express these effective Hamiltonians in a basis expanded by the following linear combination:

$$\psi_+^{(0)} = \frac{1}{\sqrt{2}}(\psi_0^{(0)} + \psi_1^{(0)}) \tag{16}$$

$$\psi_-^{(0)} = \frac{1}{\sqrt{2}}(\psi_0^{(0)} - \psi_1^{(0)}) \tag{17}$$

which are also an orthonormal basis of the truncated Hilbert space.
In this basis the truncation of H_B reads as follows,

$$H_B \longrightarrow H'_B = \begin{pmatrix} A & 0 & 0 & & \\ 0 & A & 0 & & \\ 0 & 0 & A & & \\ & & & \ddots & \\ & & & & A \end{pmatrix}, \quad A = \frac{\epsilon}{2}\begin{pmatrix} 1 & -1 \\ -1 & 1 \end{pmatrix} \tag{18}$$

with ϵ taking on the value $\epsilon^{(0)} = 1$ in the initial step of the RG-method, which is the energy of the state $\psi_1^{(0)}$.

The truncation of H_{BB} is more complicated, the result being:

$$H_{BB} \longrightarrow H'_{BB} = \begin{pmatrix} B & C & 0 & & \\ C^t & D+B & C & & \\ 0 & C^t & D+B & & \\ & & & \ddots & \\ & & & D+B & C \\ & & & C^t & D \end{pmatrix} \tag{19}$$

$$B = \begin{pmatrix} a^2 & ab \\ ab & b^2 \end{pmatrix} \quad C = \begin{pmatrix} -ab & -a^2 \\ -b^2 & -ab \end{pmatrix} \quad D = \begin{pmatrix} b^2 & ab \\ ab & a^2 \end{pmatrix}$$

with a b taking on the values $a^{(0)} = \frac{1}{\sqrt{6}} - \frac{1}{2}$ and $b^{(0)} = \frac{1}{\sqrt{6}} + \frac{1}{2}$ in the initial step of the RG-method.

The nice feature about the basis (16)-(17) is that all rows and columns of (18) and (19) add up to zero, just like the original Hamiltonians (15), implying that the constant vector is an eigenvector with zero eigenvalue of the renormalized Hamiltonian!

We shall call $H_{N/3}(\epsilon, a, b)$ the sum of the Hamiltonians (18) and (19) for generic values of ϵ, a and b. Next step in our RG-procedure is to form blocks of 4 states of the new Hamiltonian $H_{N/3}(\epsilon, a, b)$ and truncating to the two lowest $\psi_0^{(1)}$ and $\psi_1^{(1)}$ energy states within each 4-block ($4 \rightarrow 2$ truncation). The reason for this change in the number of sites per block (from 3 to 4) is motivated by the form of H'_{BB} in (19) and the fact that if we try to make a second step in the RG-method with 3-blocks the method is doomed to failure because the constant state of Fig.2 would no longer be the ground state.

Fortunately enough, with 4-blocks if we define new states $\psi_+^{(1)}$ and $\psi_-^{(1)}$ in the same form as we did in Eq.(12), we obtain that the new effective Hamiltonian is obtained by a redefinition of the parameters, namely,

$$H_{N/3}(\epsilon, a, b) \longrightarrow H_{N/6}(\epsilon', a', b') \tag{20}$$

$$\epsilon' = \frac{\epsilon}{2} + a^2 + b^2 - \Delta \tag{21}$$

$$a' = \frac{1}{2\sqrt{2}} \left[a + b - \frac{a(a^2 - 3b^2 + \Delta) + \frac{b\epsilon}{2}}{\sqrt{\Delta(\Delta + a^2 - b^2)}} \right] \tag{22}$$

$$b' = \frac{1}{2\sqrt{2}} \left[a + b + \frac{a(a^2 - 3b^2 + \Delta) + \frac{b\epsilon}{2}}{\sqrt{\Delta(\Delta + a^2 - b^2)}} \right] \tag{23}$$

$$\Delta \equiv \sqrt{(a^2 - b^2)^2 + (\frac{\epsilon}{2} - 2ab)^2} \tag{24}$$

In this fashion, the constant state of Fig.2 is again the ground state of the model and moreover, upon iteration of Eqs.(20)-(24) there are no level crossing among the excited states. Otherwise stated this means that the level structure of the block Hamiltonian H_B is preserved under the action of our BRG-method based upon the reduction from 4 to 2 states.

The energy $E_1(N)$ of the first excited state of a chain with $N = 3 \times 2^m$ sites can be obtained iterating m times Eqs.(20)-(24):

$$E_1(N = 3 \times 2^m) \equiv \epsilon^{(m)} \tag{25}$$

The initial data are given by:

$$\epsilon^{(0)} = 1, \quad a^{(0)} = \frac{1}{\sqrt{6}} - \frac{1}{2}, \quad b^{(0)} = \frac{1}{\sqrt{6}} + \frac{1}{2} \tag{26}$$

For low values of N the deviation of $\epsilon^{(m)}$ with respect to the exact result is small (see [21]). Recall that we are only keeping two states in our RG-procedure, and that the ground state energy is exactly zero by construction!. But what is more interesting about these (see [21]) is that we are able to obtain the correct size dependence, i.e., $1/N^2$ of $\epsilon^{(m)}$. As a matter of fact, the energy of the first excited state behaves for large N as (14):

$$E_1^{(exact)}(N) \sim c_{exact}/N^2, \quad \text{with} \quad c_{exact} = \pi^2 \tag{27}$$

while our BRG-method gives,

$$E_1^{(BRG)}(N) \sim c_{BRG}/N^2, \quad \text{with} \quad c_{BRG} = 12.6751 \tag{28}$$

The achievement of the $1/N^2$-law is a remarkable result which in turn allows us to match the correct order of magnitude of the energy. For instance, for 10 iterations our RG-method with 2 states kept gives the energy of the order of 10^{-6}, which is precisely the same order of magnitude as for the CBC method but with 8 states kept in the case of Fixed BC's. Recall that the standard BRG performs as bad as a 10^{-2} order of magnitude.

IV. WAVE-FUNCTION RECONSTRUCTION

Insofar we have only used our RG method to "reconstruct" the energies of the lowest states step by step, but we can also use this method to reconstruct the shape of the associate wave function in the real space. This simple fact leads to the consideration of RG applications beyond the original scope for which it was devised. As in this fashion we are making a picture of the wave function, it is natural to use the RG as a image compression method for coding images in order to facilitate its transport through the networks. For more details see the notes by Nishino in these proceedings [4].

We are able to make a reasonable picture of the first excited state wave-function based upon our BRG-procedure when compared with the exact form depicted in Fig.2. As we are working with a real-space realization of the renormalization group method, this is something we have at hand. To do this we need to perform a "reconstruction" of the wave-function. This reconstruction amounts to plot the form of our aproximate wave-function in each and every of the 3-blocks out of the 2^{m+1} in which the original chain is decomposed into under the BRG-procedure. Recall that in the initial step we started out with blocks of 3 states keeping the two lowest states $\psi_0^{(0)}$ and $\psi_1^{(0)}$ ($3 \to 2$ truncation). In the next step we make blocks of 4 states keeping the two lowest states $\psi_0^{(1)}$ and $\psi_1^{(1)}$ ($4 \to 2$ truncation) and then we perfom the iteration procedure over and over. As a result of this procedure we may express the two lowest wave functions of the $m+1$-th step in terms of those of the previous m-th step by means of the following matricial form:

$$\begin{pmatrix} \psi_0^{(m+1)} \\ \psi_1^{(m+1)} \end{pmatrix} = \frac{1}{\sqrt{2}} \begin{pmatrix} 1 & 0 \\ \alpha_m & \beta_m \end{pmatrix} \begin{pmatrix} \psi_0^{(m)} \\ \psi_1^{(m)} \end{pmatrix}_L + \frac{1}{\sqrt{2}} \begin{pmatrix} 1 & 0 \\ -\alpha_m & \beta_m \end{pmatrix} \begin{pmatrix} \psi_0^{(m)} \\ \psi_1^{(m)} \end{pmatrix}_R \tag{29}$$

where the LHS of Eq. (29) represents the wave function of $3 \times 2^{m+1}$ sites while in the RHS we have a left-wave-function of 3×2^m sites and another right-wave-function of 3×2^m sites, so that everything squares. The parameters appearing in Eq. (29) turn out to be given by:

$$\alpha_m = \frac{(\frac{\epsilon_m}{2} - 2a_m b_m) + (a_m^2 - b_m^2 + \Delta_m)}{2\sqrt{\Delta_m(\Delta_m + a_m^2 - b_m^2)}} \tag{30}$$

$$\beta_m = \frac{(\frac{\epsilon_m}{2} - 2a_m b_m) - (a_m^2 - b_m^2 + \Delta_m)}{2\sqrt{\Delta_m(\Delta_m + a_m^2 - b_m^2)}} \tag{31}$$

with Δ_m as in Eq.(24). Their initial values are $\alpha_0 = 1/\sqrt{10}$ and $\beta_0 = 3/\sqrt{10}$.
We may recast Eq. (29) in more compact form by writing:

$$\Psi^{(m+1)} = L_m \Psi_L^{(m)} + R_m \Psi_R^{(m)} \tag{32}$$

where

$$L_m = \frac{1}{\sqrt{2}} \begin{pmatrix} 1 & 0 \\ \alpha_m & \beta_m \end{pmatrix}, \quad R_m = \frac{1}{\sqrt{2}} \begin{pmatrix} 1 & 0 \\ -\alpha_m & \beta_m \end{pmatrix} \tag{33}$$

We may call Eq.(32) the *reconstruction equation*. This is the master equation that when iterated "downwards" (reconstruction) allows us to obtain the picture of our approximate BRG-wave-function corresponding to every and each block of 3 sites of the 2^{m+1} blocks in which the chain is decomposed into. At the end of the iteration procedure we end up with expressions for the values of the 3-sites wave-functions in terms of the initial two lowest states $\psi_0^{(0)}$ and $\psi_1^{(0)}$. The first one is a constant function while the second is a straight line of negative slope. Thus, these two states turn out to be the building blocks of our BRG-procedure.

When using the reconstruction equation to obtain the wave function we may use a binary code based upon the labels L (left) and R (right) to keep track of the different 3-sites

blocks which make up the chain. Thus, in one dimension the RG-blocks are in a one-to-one correspondence with a binary numerical system. In general, for other dimensions we may state squematically the following correspondence:

$$\text{BRG-prescription} \longleftrightarrow \text{“Number System”}$$

This simple observation is the basis of a coding system for compressing pictures whatever may be its origin. In two dimensions we need more digits to make the coding, but it works likewise and serves for image compression [4].

V. THE CORRELATED BLOCK RENORMALIZATION GROUP (CBRG)

We have already mentioned in the Introduction that the DMRG is not only a powerful computational method but also a source of inspiration for further works concerning the RG. For these reasons, it is worthwhile to explore different options or alternatives to the DMRG which may be useful in situations where the DMRG encounters difficulties, as in the case of 2D quantum systems. The main message of the DMRG is that blocks are correlated. The implementation of this idea by means of the density matrix formalism may be not the unique way to proceed. On the other hand, the “onion-scheme” a la Wilson adopted by the DMRG, while being one of the reasons of its spectacular accuracy, imposes certain limitations.
At this stage it is not clear how fundamental are the density-matrix formalism or the onion-scheme for a RG method which takes into account the correlation between blocks. One can indeed combine the Kadanoff block method with the use of a density matrix in the process of truncation, as in reference [12]. More work remains to be done to see wheather there is a real improvement of the standard BRG method by combining it with the DMRG as in [12]. In this section we want to explore another possibility which is to give up both the density matrix and the onion-scheme (see [22]). With this point of view in mind, it would seem that we should come pretty close to the standard BRG method, were it not for the enormous freedom hidden in a Real-Space RG method. This freedom comes from the separation of the

Hamiltonian into an intrablock H_B and an interblock H_{BB} Hamiltonian. This is a source of ambiguities which can be sometimes mitigated with the aide of symmetry arguments, but not fully eliminated though. This ambiguity shows up specially for terms in the Hamiltonian acting at the boundaries of the block. There are no general criteria as to how to include this type of terms either into the intrablock or into the interblock Hamiltonians, or into both! For example, in the 1D Ising model in a transverse field (ITF model), a choice which preserves the selfduality of the model attributes some self-couplings to the H_B and others to the interblock H_{BB}, and it yields to an exact value of the critical point and the critical exponent ν [23], [15]. The ambiguity in the splitting of H into the sum $H_B + H_{BB}$ thus affect deeply the truncation procedure itself, which is based on the diagonalization of H_B. Rather than blaming the BRG for its lack of uniqueness, we should use its freedom to allow the blocks to become correlated in the RG procedure. In our present approach this correlation will be taken into account in a "dynamical" way rather than in a "statistical" way as in the DMRG. This will be achieved by the introduction of interblock operators which reflect the "influence" between neighbour blocks and which are defined at the boundary of the block in the first step of our CBRG method.

We have chosen to illustrate our approach the 1D and 2D tight-binding models mainly for simplicity reasons, but we believe that our method could be applied to more complicated problems. In fact, the first step in this direction was already undertaken in reference [21], where only 2 states at each stage of the RG-blocking were retained. This in turn allowed us to obtain the $1/N^2$ scaling law for the size dependence of the first-excited-state energy.

We shall give the general mathematical structure underlying the results of reference [21]. This will allow us to retain more than two states in the RG-truncation and also to consider the two-dimensional tight-binding model. In this fashion, we shall recover the n^2/N^2 scaling law for the n-th excited state of the 1D model and the scaling law $\frac{n_1^2+n_2^2}{N^2}$ in the 2D case. These results will then show that the CBRG method describes correctly the low energy behaviour of the 1D and 2D Laplacian.

VI. THE CBRG METHOD: ONE DIMENSION

The problem we want to study is the one-dimensional Tight-Binding model in an open chain with different boundary conditions at its ends. The Hamiltonian for this system takes the following matricial form,

$$H_{b,b'} = \begin{pmatrix} b & -1 & & & & \\ -1 & 2 & -1 & & & \\ & -1 & 2 & & & \\ & & & \ddots & & \\ & & & & 2 & -1 \\ & & & & -1 & b' \end{pmatrix} \tag{34}$$

where b and b' take on the values 1 (or 2) corresponding to Free (or Fixed) BC's respectively. This Hamiltonian is the discrete version of the Laplacian $H = -\partial_x^2$, while the Free or Fixed BC's correspond in the continuum to the vanishing of the wave function (Fixed BC's) or its spatial derivative (Free BC's) at the ends of the chain, i.e.,

$$\begin{aligned} b = 2 \;&\Rightarrow\; \Psi(0) = 0 \quad \text{Fixed BC} \\ b = 1 \;&\Rightarrow\; \tfrac{\partial \Psi}{\partial x}(0) = 0 \quad \text{Free BC} \end{aligned} \tag{35}$$

and similarly for b' which contains the BC at the other end of the chain.
Hence, altogether there are 4 Hamiltonians of the type in (34), whose eigenstates and eigenvalues are the subject of our RG-techniques.

The first step in the RG method is to divide the lattice into blocks containing n_s sites each and labeled with and index p $(= 1, \ldots, N/n_s)$. Let us suppose for a moment that we isolate the pth-block from the rest of the lattice so that its dynamics, as an independent entity, is governed by a Hamiltonian denoted by A_p, which we may call *uncorrelated block Hamiltonian*. The restoration of the block back into the lattice involves two effects. The first one is that the BC's of the p-th block may change under the influence of the $p+1$ and $p-1$ blocks. We describe this change of BC's by the action of *Boundary Operators* denoted

by $B_{p,p\pm1}$ on the pth-block. The second effect is the interaction between the pth-block and its neighbours $p+1$ and $p-1$, given by interaction Hamiltonians $C_{p,p\pm1}$ which act on both p and $p+1$ blocks simultaneously. If the problem under consideration is translationally invariant, all the Hamiltonians defined above are independent of the block label p, in which case we denote them by,

$$\begin{aligned} A_p &= A \\ B_{p,p+1} = B_R \quad & B_{p,p-1} = B_L \\ C_{p,p+1} = C \quad & C_{p,p-1} = C^\dagger \end{aligned} \tag{36}$$

The $H_{Free,Free}$ Hamiltonian (34) gives an example of this as we shall show below. Hence, for the time being, we shall consider the situation described by (36) and leave the more general case after explaining the general ideas.

In the standard BRG method the block Hamiltonian H_B and the interblock Hamiltonian H_{BB} are given, according to our previous definitions, by the following formulas

$$H_B = A + B_L + B_R \tag{37}$$

$$H_{BB} = \begin{pmatrix} 0 & C \\ C^\dagger & 0 \end{pmatrix} \tag{38}$$

The whole Hamiltonian is by all means the sum of H_B and H_{BB} for all the blocks of the chain.

Next step in the RG method is to diagonalize H_B and keep its, say m ($m < n_s$), lowest eigenstates. The truncation is given by a $n_s \times m$ matrix T whose columns are precisely the components of the m lowest eigenstates of H_B. The renormalized Hamiltonian in the new basis is given by,

$$H' = T^\dagger (H_B + H_{BB}) T \tag{39}$$

At first sight from Eq. (37) it would seem that we have taken into account the effect of the BC's on a given block. However, as the examples show, this is quite a bit illusory.

On the other hand, the distinction among A, B_L and B_R is rather inmaterial as far as H_B is concerned, and in fact no distinction of this sort is made in the standard BRG formalism. Finally, let us observe that H_B and H_{BB} play rather different roles in the truncation procedure. This asymmetry has been observed as a source of problems by several authors in the past [23], [20].

We shall mention that this asymmetry has recently been related to quantum groups in a fashion which has led to a new RG method called the Renormalization Quantum Group method [15], [16].

Therefore, from various points of view, one is urged to make more explicit the role played by the BC-operators B_L and B_R in our CBRG procedure. For this purpose, we have found convenient to use the concept of superblock already introduced in reference [17]. We shall define a superblock as the set of two consecutive blocks, p and $p+1$ and denoted by $(p, p+1)$. The great advantage of the superblock is that it allows us to materialize the distinction among A, B_L and B_R . In fact, just as the isolation of a single block leads us to the definition of the Hamiltonian A, the isolation of two blocks contained in a superblock allows us to define B_L, B_R and also C through the superblock Hamiltonian H_{sB} as follows,

$$H_{sB} = \begin{pmatrix} A + B_R & C \\ C^\dagger & A + B_L \end{pmatrix} \tag{40}$$

Similarly, the Hamiltonian describing the interaction between superblocks is given by (see Fig.4)

$$H_{sB,sB} = \begin{pmatrix} 0 & & & \\ & B_R & C & \\ & C^\dagger & B_L & \\ & & & 0 \end{pmatrix} \tag{41}$$

Now instead of diagonalizing H_B in Eq. (37), in the CBRG method we shall diagonalize H_{sB} in Eq. (40), and afterwards keep the $m = n_s$ lowest eigenstates in the tight-binding model. As in the standard BRG method, the change to the truncated basis defines the renormalized operators as follows:

$$H_{sB} \longrightarrow T^{\dagger} H_{sB} T = A' \tag{42}$$

$$H_{sB,sB} \longrightarrow T^{\dagger} H_{sB,sB} T = \begin{pmatrix} B'_R & C' \\ C'^{\dagger} & B'_L \end{pmatrix} \tag{43}$$

where the matrices A',B'_R, B'_L and C' are the renormalized version of the operators A,B_R, B_L and C, and they exhibit the same geometrical interpretation for the renormalized block as their unprimed partners for the original blocks.

If we set $B_R = B_L = 0$ in Eqs. (40) and (41), then after the first RG-step we get $B'_R = B'_L = 0$ and thus the previous RG-scheme coincides with the standard BRG. We may say that uncorrelated blocks are in a sense a fixed point of our method. However, this fixed point may be unstable, and to explore this possibility one has to look for non-vanishing B-operators and their RG-evolution.

Let us address now some examples. We shall first study the Hamiltonian (34) with Free BC's at the ends ($b = b' = 1$). Choosing $n_s = 3$ for example, we see that the choice for the operators A,B_R, B_L and C in the first step of the CBRG procedure is given by,

$$A = \begin{pmatrix} 1 & -1 & 0 \\ -1 & 2 & -1 \\ 0 & -1 & 1 \end{pmatrix}, \; B_R = \begin{pmatrix} 0 & & \\ & 0 & \\ & & 1 \end{pmatrix}, \; B_L = \begin{pmatrix} 1 & & \\ & 0 & \\ & & 0 \end{pmatrix}, \; C = \begin{pmatrix} 0 & 0 & 0 \\ 0 & 0 & 0 \\ -1 & 0 & 0 \end{pmatrix} \tag{44}$$

This choice is equivalent to the assumption that an isolated block satisfies Free BC's at its ends. The role of B_R and B_L is to *join* these blocks into a single chain. This is the *geometrical* explanation of Eqs. (44). In more general cases one must have to explore which is the best choice. The generalization of Eqs.(44) to blocks with more than 3 sites is obvious. In Table 1 we collect our CBRG-results for the first 5 excited states for a chain of $N = 12 \times 2^6 = 768$ sites. Comparison with exact results gives a good agreement.

An important feature of our CBRG method is that the n^2/N^2- scaling law ($N \longrightarrow \infty$) for the energy of the n-excited states of a chain made up of N sites, is reproduced correctly (see Fig.5). In Table 2 we show the variation of the first-excited-state energy with the size

N of the chain. From those values we can extract the corresponding $1/N^2$-law which turns out to be,

$$E_1^{(CBRG)}(N) = c_{CBRG}^{(1)} \frac{1}{N^2}, \quad c_{CBRG}^{(1)} = 9.8080, \ (N \longrightarrow \infty) \text{ Free-Free BC's} \tag{45}$$

while the exact value for the proportionality constant c is $c_{\text{exact}} = \pi^2 = 9.86$. This amounts to a 0.6 % error.

Likewise, we have enough data so as to obtain the corresponding n^2/N^2-law for the whole set of 5 excited states. Thus, the scaling law we obtain is,

$$E_n^{(CBRG)}(N) = c_{CBRG} \frac{n^2}{N^2}, \quad c_{CBRG} = 8.4733, \ (N \longrightarrow \infty) \text{ Free-Free BC's} \tag{46}$$

which now amounts to a 7.34 % error. This is a natural fact from the worse knowledge of the highest excited states of the spectrum in a RG-scheme.

We can make even more explicit the successful achievement of the $1/N^2$-scaling law by leaving as a free adjustable parameter the exponent of $1/N$ in addition to the proportionality constant. Let us denote by θ this critical exponent. Using data from 20 to 50 steps of our CBRG-method for several truncation of states according to our scheme $2n_s \rightarrow n_s$ (namely, $n_s = 10, 13, 20$) we arrive at the following results,

$$E_1^{(CBRG)}(N) = c_{CBRG} \frac{1}{N^\theta}, \quad (N \longrightarrow \infty) \text{ Free-Free BC's} \tag{47}$$

$$\begin{aligned} &\text{For} \ \ 20 \longrightarrow 10 \quad \theta = 1.9708 \\ &\text{For} \ \ 26 \longrightarrow 13 \quad \theta = 1.9734 \\ &\text{For} \ \ 40 \longrightarrow 20 \quad \theta = 1.9854 \end{aligned} \tag{48}$$

These results clearly support the fact that we have correctly reproduced the exact value of $\theta = 2$ for the finite-size critical exponent.

Last, but not least, as was proved in [21] our CBRG method gives the *exact* energy of the ground state for every step of the RG-procedure for Free-Free BC's.

In tables 1 and 2 we also show the results we have obtained with a DMRG analysis following White's method [1]. This analysis is based on the onion scheme of enlarging the lattice site

by site á la Wilson. The results coincide with the exact values within the 4 digits precision used here, but they start differing when keeping more digits. Nevertheless, the DMRG is much more time consuming than our CBRG method for it has to build the lattice site by site, while the CBRG reproduces the lattice by blocking which is much more efficient as far as CPU time is concern, and moreover, it applies to two-dimensional situations where the onion scheme fails to reproduce the lattice. We have also performed the DMRG analysis in 1D for Fixed-Fixed BC's in table 4 where the same considerations apply.The CBRG method is also more suitable for analytic formulations [21].

In reference [21] it was shown that one can reproduce easily the wave function of the excited states. This procedure was called *reconstruction* since it works "downwards" in the CBRG method. The basic equation to be used is the *reconstruction equation* [21],

$$\Psi^{(r+1)} = L_r \Psi_L^{(r)} + R_r \Psi_R^{(r)} \tag{49}$$

where $\Psi^{(r)}$ denotes the collection of m lowest eigenstates in the r-step of the CBRG-procedure, and L_r, R_r are the block matrices in terms of which the truncation matrix $T^\dagger$ can be written as $T^\dagger = (L_r, R_r)$.

Our results for a chain of $N = 12 \times 2^6 = 768$ sites and $n_s = 6$ states kept are given in Fig.6 where we have plotted the first 5 excited states and compare them with the exact wave functions. There are some remarkable facts regarding these figures. Firstly, the number of nodes is correctly preserved by our CBRG wave functions. Secondly, the Free-Free type of boundary conditions are also correctly reproduced at the ends of the chain. And lastly, it is worthwhile to point out that the CBRG wave functions "degrade gracefully" as the energy of the excited state raises in accordance with the fact that the lower the energy is, the more reliable are the results.

This ends the results for the Free-Free BC's. In order to address other types of BC's we must come back to the case where the matrices A,B_R, B_L and C depend on each particular block. Thus, for example, for the Fixed-Free BC's we shall choose as the uncorrelated A-matrix for the block located to the left end of the chain the following form ($n_s = 3$),

$$A_1 = \begin{pmatrix} 2 & -1 & 0 \\ -1 & 2 & -1 \\ 0 & -1 & 1 \end{pmatrix} \quad \text{Fixed-Free BC's} \tag{50}$$

while the remaining matrices A_p, $(p = 2, \ldots, N/3)$, will be given by Eqs.(36), (44).

For Free-Fixed BC's, it is the last A-matrix which we have to take different from the others, namely,

$$A_{N/3} = \begin{pmatrix} 1 & -1 & 0 \\ -1 & 2 & -1 \\ 0 & -1 & 2 \end{pmatrix} \quad \text{Free-Fixed BC's} \tag{51}$$

As for the Fixed-Fixed BC's case, we must change the A-matrix at both ends of the chain according to the following prescription,

$$A_1 = \begin{pmatrix} 2 & -1 & 0 \\ -1 & 2 & -1 \\ 0 & -1 & 1 \end{pmatrix}, \quad A_{N/3} = \begin{pmatrix} 1 & -1 & 0 \\ -1 & 2 & -1 \\ 0 & -1 & 2 \end{pmatrix} \quad \text{Fixed-Fixed BC's} \tag{52}$$

Then we follow the same steps as for the Free-Free BC's, taking care that the A,B_R, B_L and C matrices in each CBRG-step may depend on the position of the blocks. This implies in particular that the embedding T-matrices may also vary from block to block.

In Tables 3 and 4 we summarize our results for the Free-Fixed and Fixed-Fixed BC's (Fixed-Free BC's are equivalent to Free-Fixed BC's by parity transformation). In these tables we present our CBRG results for the first 6 lowest lying states for the 1D tight-binding model in a chain of $N = 12 \times 2^5 = 384$ sites with mixed boundary conditions, and they are compared against the exact and standard BRG values. Several remarks are in order. First, we observe that the CBRG method produces a good agreement with the exact results and certainly much more accurate by several orders of magnitude than the old BRG method. Second, the CBRG method is able to reproduce the corresponding n^2/N^2-scaling laws for the spectrum of excited states in each case of mixed BC's. Namely,

- For Free-Fixed BC's and considering just the ground state, we have

$$E_0^{(CBRG)}(N) = c_{CBRG}^{(0)} \frac{1}{4N^2}, \quad c_{CBRG}^{(0)} = 9.072, \ (N \longrightarrow \infty) \text{ Free-Fixed BC's} \tag{53}$$

  which amounts to a 8 % error with respect to the exact value of $c_{exact} = \pi^2$.

  As for the corresponding law for the whole spectrum, we find

$$E_n^{(CBRG)}(N) = c_{CBRG} \frac{(n+1)^2}{4N^2}, \quad c_{CBRG} = 7.6729, \ (N \longrightarrow \infty) \text{ Free-Fixed BC's} \tag{54}$$

  which represents a 11.5 % error with respect to the exact value of π^2.

- For Free-Fixed BC's and considering just the ground state, we have

$$E_0^{(CBRG)}(N) = c_{CBRG}^{(0)} \frac{1}{N^2}, \quad c_{CBRG}^{(0)} = 8.35, \ (N \longrightarrow \infty) \text{ Fixed-Fixed BC's} \tag{55}$$

  which amounts to a 8 % error with respect to the exact value of $c_{exact} = \pi^2$.

  As for the corresponding law for the whole spectrum, we find

$$E_n^{(CBRG)}(N) = c_{CBRG} \frac{(n+1)^2}{N^2}, \quad c_{CBRG} = 6.9696, \ (N \longrightarrow \infty) \text{ Fixed-Fixed BC's} \tag{56}$$

  which represents a 16 % error with respect to the exact value of π^2.

We obtain bigger errors in the determination of these scaling laws as compared with the Free-Free case mainly because we have used less data in our fitting. Nevertherless, we find a good agreement with the exact results. Yet, there is another reason as to why the accuracy in the case of mixed BC's is worse, namely, the ground state wave function Ψ_0 is not homogeneous in space as it is in the Free-Free case [21]. This makes the RG-procedure more involved and a source of extra uncertainties.

Let us mention in passing that we are also able to make a wave function reconstruction in the mixed BC's cases as has been done for the Free-Free BC case.

The outcome of all the results presented so far is that we have succeded in devising a Real-Space RG method capable of reproducing the correct eigenvalues and eigenstates for

the tight-binding model as originally envisaged by Wilson, within a certain accuracy which can in principle be improved.

Althoug the model we have employed to test our CBRG-method is a tight-binding model, there are some remarkable facts regarding the fixed-point structure of our CBRG-solution that we would like to stress. Namely, we have found that after enough number of CBRG-iterations, the matrices A, B_L, B_R and C in the Free-Free case scale nicely with the size N of the chain according to the dynamical critical exponent z. To be more precise, let us introduce the fixed point values of those matrices denoted by A^*, B_L^*, B_R^* and C^* which we define as,

$$A^* = N^{-z}a^*, \quad B_L^* = N^{-z}b_L^*, \quad B_R^* = N^{-z}b_R^*, \quad C^* = N^{-z}c^*, \quad \text{Fixed-Point values} \tag{57}$$

in terms of the scaled matrices a^*, b_L^*, b_R^* and c^*. For a block of 3 sites ($n_s = 3$) we find the following Fixed-Point structure parametrized by two constants s and t (for bigger n_s we need extra parameters),

$$a^* = 0,\ b_R^* = \begin{pmatrix} 1 & s & s \\ s & t & t \\ s & t & t \end{pmatrix},\ b_L^* = \begin{pmatrix} 1 & -s & s \\ -s & t & -t \\ s & -t & t \end{pmatrix},\ c^* = \begin{pmatrix} -1 & s & -s \\ -s & t & -t \\ -s & t & -t \end{pmatrix} \tag{58}$$

with $s = 1.3993$ and $t = 1.9581$. The critical exponent z we obtain is,

$$z = 0.9999 \tag{59}$$

which is indeed very close to the exact value $z = 1$ (actually, it differs in the ninth decimal digit).

The interpretation of this Fixed-Point in the context of the CBRG method is as follows. We pointed out before that when the boundary operators $b_{L,R}$ vanish we recover the standard BRG method in which the blocks are not correlated. Here we find that it is the uncorrelated Hamiltonian which vanish, while the boundary $b_{L,R}$ and interaction c operators do not vanish within the scaling law. This fact may perhaps be interpreted by saying that in the example under study the correlation between blocks is more important than their selfenergy. In

references [25], [26], [27] it was shown that the DMRG method leads, in the thermodynamic limit, to a "product form" ansatz for the ground state wave function. In our case we see from Eqs.(57), (58) that we also reach thermodynamical limit, which leads us to ask about the nature of the ansatz for the ground state and excited states implied by the CBRG method. The answer to this question will be addressed in a future publication but it suffices to say that both the DMRG and the CBRG methods seem to yield different ansatzs of the ground state wave function. In a few words, the DMRG is associated with a "vertex picture" while the CBRG is associated with a "string picture".

VII. THE TWO-DIMENSIONAL CBRG-ALGORITHM

The RG-method that we have devised in the one-dimensional problem can be generalized in a natural way to higher dimensions. We shall consider for simplicity the 2D case. First of all, we divide the square lattice into blocks of n_s sites each. Each block will in turn be a square lattice with a minimum of 4 sites ($= 2 \times 2$ block). As in 1D, we shall define the following Hamiltonians to carry out the CBRG-program,

- A_p = self-energy of the p-th block isolated from the lattice.
- $B_{p,q}$ = self-energy of the p-th block induced by the presence of the q-th block.
- $C_{p,q}$ = interaction between the p-th block and the q-th block.

The difference with respect to the 1D case is that each block has now 4 neighbours and therefore there are four different B and C matrices.

Let us consider again the Hamiltonian of a free particle moving in a 2D-box with Free BC's at the boundaries of the box. The 2D Hamiltonian is given again by the incidence matrix of the lattice. As in 1D we shall choose the matrix A as the incidence matrix of the block. Thus, for example, for a 2×2 block we have,

$$A = \begin{pmatrix} 2 & -1 & 0 & -1 \\ -1 & 2 & -1 & 0 \\ 0 & -1 & 2 & -1 \\ -1 & 0 & -1 & 2 \end{pmatrix} \tag{60}$$

The 4 Boundary Operators B have a diagrammatic representation [22] which helps us to keep track of their location in the block H_B and interblock H_{BB} Hamiltonians. Their explicit matricial form is as follows,

$$B_{12} = B_{43} = B_L = \begin{pmatrix} 0 & & & \\ & 1 & & \\ & & 1 & \\ & & & 0 \end{pmatrix}, \quad B_{21} = B_{34} = B_R = \begin{pmatrix} 1 & & & \\ & 0 & & \\ & & 0 & \\ & & & 1 \end{pmatrix} \tag{61}$$

$$B_{14} = B_{23} = B_D = \begin{pmatrix} 0 & & & \\ & 0 & & \\ & & 1 & \\ & & & 1 \end{pmatrix}, \quad B_{41} = B_{32} = B_U = \begin{pmatrix} 1 & & & \\ & 1 & & \\ & & 0 & \\ & & & 0 \end{pmatrix} \tag{62}$$

where the labels denote the position of the neighbouring blocks and we have used the translation invariance of the 2D tight-binding model so that we need only to distinguish between Right and Left, and Up and Down.

As for the Interaction C-Operators [22] we have the following matricial representation, with the same considerations as for the B-operators,

$$C_{12} = C_{43} = C_{LR} = \begin{pmatrix} 0 & 0 & 0 & 0 \\ -1 & 0 & 0 & 0 \\ 0 & 0 & 0 & -1 \\ 0 & 0 & 0 & 0 \end{pmatrix}, \quad C_{21} = C_{34} = C_{RL} = \begin{pmatrix} 0 & -1 & 0 & 0 \\ 0 & 0 & 0 & 0 \\ 0 & 0 & 0 & 0 \\ 0 & 0 & -1 & 0 \end{pmatrix} \tag{63}$$

$$C_{14} = C_{23} = C_{DU} = \begin{pmatrix} 0 & 0 & 0 & 0 \\ 0 & 0 & 0 & 0 \\ 0 & -1 & 0 & 0 \\ -1 & 0 & 0 & 0 \end{pmatrix}, \quad C_{41} = C_{32} = C_{UD} = \begin{pmatrix} 0 & 0 & 0 & -1 \\ 0 & 0 & -1 & 0 \\ 0 & 0 & 0 & 0 \\ 0 & 0 & 0 & 0 \end{pmatrix} \tag{64}$$

Thus translation invariance reduces the number of independent CBRG-matrices by a half. These relations are particular of the problem at hand but we must left open the posibility of having all those matrices different from each other in order to handle more complicated problems.

Now that we have all the elements entering in our CBRG-method we proceed to construct the block H_{sB} and interblock $H_{sB,sB}$ Hamiltonians out of them. To this end we have to consider a superblock made up of 4 blocks [22]. Thus, for H_{sB} we have,

$$H_{sB} = \begin{pmatrix} A + B_L + B_D & C_{LR} & 0 & C_{DU} \\ C_{RL} & A + B_R + B_D & C_{DU} & 0 \\ 0 & C_{UD} & A + B_R + B_U & C_{RL} \\ C_{UD} & 0 & C_{LR} & A + B_L + B_U \end{pmatrix} \tag{65}$$

This is a $4n_s \times 4n_s$ matrix made up of $n_s \times n_s$ matrices.

As for the interblock Hamiltonian $H_{sB,sB}$ we have to distinguish between (sB, sB)-couplings of horizontal type denoted by $H^{(hor)}_{sB,sB}$ and vertical type denoted by $H^{(ver)}_{sB,sB}$, which read explicitly as,

$$H^{(hor)}_{sB,sB} = \begin{pmatrix} B_R & & & 0 & C_{RL} & 0 & 0 \\ & 0 & & 0 & 0 & 0 & 0 \\ & & 0 & 0 & 0 & 0 & 0 \\ & & & B_R & 0 & 0 & C_{RL} & 0 \\ 0 & 0 & 0 & 0 & 0 & & & \\ C_{LR} & 0 & 0 & 0 & & B_L & & \\ 0 & 0 & 0 & C_{LR} & & & B_L & \\ 0 & 0 & 0 & 0 & & & & 0 \end{pmatrix}, \quad H^{(ver)}_{sB,sB} = \begin{pmatrix} B_D & & & 0 & 0 & 0 & C_{UD} \\ & B_D & & 0 & 0 & C_{UD} & 0 \\ & & 0 & 0 & 0 & 0 & 0 \\ & & & 0 & 0 & 0 & 0 & 0 \\ 0 & 0 & 0 & 0 & 0 & & & \\ 0 & 0 & 0 & 0 & & 0 & & \\ 0 & C_{DU} & 0 & 0 & & & B_U & \\ C_{DU} & 0 & 0 & 0 & & & & B_U \end{pmatrix} \tag{66}$$

where we have made use again of translational invariance.

Once that we have made our choice for the decomposition of the total Hamiltonian of the 2D-tight-binding model into block and interblock Hamiltonians according to our CBRG-prescription, we can carry on with the truncation part of the RG-method. We shall keep n_s states out of $4n_s$ states per superblock so that our truncation scheme may be summarized as,

$$4n_s \text{ (superblock)} \longrightarrow n_s \text{ (new block)}$$

Recall that at each step of the CBRG-method we need to identify the A, B_L, B_R and C operators which define the truncation procedure for the next step of the method. For this purpose, firstly the truncation of the superblock H_{sB} gives rise to the A' uncorrelated self-energy operator for the next RG-step, namely,

$$H_{sB} \text{ (} 4n_s \times 4n_s \text{ matrix)} \longrightarrow A' \text{ } (n_s \times n_s \text{ matrix}) \tag{67}$$

To identify the rest of the operators we have to renormalize the interblock Hamiltonian which comes in two types, horizontal and vertical. The renormalization of the $H^{(hor)}_{sB,sB}$ Hamiltonian is given by [22],

$$H^{(hor)}_{sB,sB} \longrightarrow \begin{pmatrix} B'_R & C'_{RL} \\ C'_{LR} & B'_L \end{pmatrix} \tag{68}$$

Likewise, for the $H^{(ver)}_{sB,sB}$ Hamiltonian we have,

$$H^{(ver)}_{sB,sB} \longrightarrow \begin{pmatrix} B'_D & C'_{UD} \\ C'_{DU} & B'_U \end{pmatrix} \tag{69}$$

Now that we have identified all the operators defining the CBRG method at the new stage of the renormalization, we may reconstruct the new superblock Hamiltonian H'_{sB}, which in turn has the same form as the original H_{sB} in Eq.(65) substituting all the operators by their *primed versions*. This statement can be explicitly checked by considering the set of 4 superblocks [22]. Firstly, the new H'_{sB} has a contribution coming from the truncation of each of the 4 superblocks, each of them contributing with an A'-operator as in Eq.(67). Secondly, H'_{sB} picks up two more contributions coming from the horizontal and vertical interaction between superblocks, which we denote by $H_{\leftrightarrow}$ and $H_{\updownarrow}$. Thus, in the CBRG-method H'_{sB} is renormalized as,

$$H'_{sB} = \begin{pmatrix} A' & & & \\ & A' & & \\ & & A' & \\ & & & A' \end{pmatrix} \longleftarrow \text{(single superblock contribution)}$$

$$(H_{\leftrightarrow}) \;\rightarrow\; + \begin{pmatrix} B'_L & C'_{LR} & & \\ C'_{RL} & B'_R & & \\ & & 0 & \\ & & & 0 \end{pmatrix} + \begin{pmatrix} 0 & & & \\ & 0 & & \\ & & B'_R & C'_{RL} \\ & & C'_{LR} & B'_L \end{pmatrix}$$

$$(H_{\updownarrow}) \;\rightarrow\; + \begin{pmatrix} B'_U & & C'_{DU} & \\ & 0 & & \\ & & 0 & \\ C'_{UD} & & B'_D & \end{pmatrix} + \begin{pmatrix} 0 & & & \\ & B'_U & C'_{DU} & \\ & C'_{UD} & B'_D & \\ & & & 0 \end{pmatrix} \tag{70}$$

and altogether we arrive at the previously stated result of Eq.(65).

Similarly we may proceed with the renormalized interblock Hamiltonians $H'^{(hor)}_{sB,sB}$ (68) and $H'^{(ver)}_{sB,sB}$ (69) and we end up with the same form for them as the original ones.
This ends the implementation of the CBRG-method for the 2D-tight-binding model.

In Table 5 we collect our CBRG results for the first 4 lowest lying states for a chain of $N = 4 \times 4 \times 4^6 = 65536$ sites. Comparison with the exact results gives a good agreement. We have also data from truncations with blocks of $n_s = 9$ and $n_s = 16$ sites which enforce this statement. Moreover, notice that the first excited state is a doublet as in the exact solution.

Another important result of our CBRG-method is that the $(n_1^2 + n_2^2)/N^2$ scaling law for the energy of the (n_1, n_2)-excited states of a square lattice of length N is reproduced correctly. In fact, from data of the $n_s = 16$ sites truncation for the first-excited-state energy we can extract the corresponding $1/N^2$-scaling law which turns out to be,

$$E_1^{(CBRG)}(N) = c^{(1)}_{CBRG}\frac{1}{N^2}, \quad c^{(1)}_{CBRG} = 9.7365, \ (N \longrightarrow \infty) \text{ D=2 Free BC's} \tag{71}$$

while the exact value of the proportionality constant c is $c_{exact} = \pi^2 = 9.86$. This amounts to a 1.3 % error.

Likewise, we may obtain the full $(n_1^2 + n_2^2)/N^2$ scaling law for the whole set of 15 excited states and we find,

$$E^{(CBRG)}_{(n_1,n_2)}(N) = c^{(1)}_{CBRG}\frac{(n_1^2 + n_2^2)}{N^2}, \quad c_{CBRG} = 7.9074, \ (N \longrightarrow \infty) \text{ D=2 Free BC's} \tag{72}$$

which now amounts to a 10.5 % error.

As in the 1D Free-Free case, we can determine critical scaling exponent θ (47). For a truncation scheme $16 \rightarrow 4$ we find,

$$\theta = 1.99999981 \quad \text{D=2} \tag{73}$$

which clearly supports the scaling laws introduced above. Notice again (see Table 5) that our CBRG method gives the exact (within machine precision) energy of the ground state. This is true for every step of the RG, as was proved in [21] for 1D.

We can also perform the wave function reconstruction of the excited states in the two-dimensional real space. This is achieved by a two-dimensional extension of the reconstruction equation (49). As an illustration of how the CBRG method performs with this matter, see [22]. The qualitative real-space form of the excited-state wave functions are captured by the CBRG procedure.

With this discussion we close the first part of these notes which have been devoted to new develoments of the Real-Space RG method revolving around the new ideas brought about by the Density Matrix RG method.

VIII. STANDARD BRG FOR THE 1D AF HEISENBERG MODEL

In the remaining sections we shall return to the standard BRG methods to deal in an analytical controlled fashion with models which include many-body interactions unlike the free models considered in the first part of these notes.

The arquetypical model we shall be dealing with is the Heisenberg model which will be studied in ladder systems and 2D lattices (square, honeycomb). Our point will be that even with the old-fashion BRG can be useful to retrieve the correct qualitative phyisics when properly implemented. To this end we shall be needing some results concerning the Heisenberg model in one dimension which will be basic.

Let us recall the standard BRG method for the AF Heisenberg-Ising model whose Hamiltonian is given by:

$$H_N = J \sum_{j=1}^{N-1} (S_j^x S_{j+1}^x + S_j^y S_{j+1}^y + \Delta S_j^z S_{j+1}^z) \tag{74}$$

where $\Delta \geq 0$ is the anisotropic parameter and $J > 0$ for the antiferromagnetic case. If $\Delta = 1$ one has the AF-Heisenberg model which was solved by Bethe in 1931. If $\Delta = 0$ one has the XX-model which can be trivially solved using a Jordan-Wigner transformation which maps it onto a free fermion model. For the remaing values of Δ the model is also solvable by Bethe ansatz and it is the 1D relative of the 2D statistical mechanical model known as the 6-vertex or XXZ-model.

The region $\Delta > 1$ is massive with a doubly degenerate ground state in the thermodynamic limit $N \to \infty$ characterized by the non-zero value of the staggered magnetization,

$$m_{\rm st} = \langle \frac{1}{N} \sum_j S_j^z (-1)^j \rangle \tag{75}$$

The region $0 \leq \Delta \leq 1$ is massless and the ground state is non-degenerate with a zero staggered magnetization. The phase transition between the two phases has an essential singularity.

We would like next to show which of these features are captured by a real-space RG-analysis. The rule of thumb for the RG-approach to half-integer spin model or fermion model is to consider blocks with an *odd number of sites*. This allows in principle, although not necessarilly, to obtain effective Hamiltonians with the same form as the original ones. Choosing for (74) blocks of 3 sites we obtain the block Hamiltonian:

$$\frac{1}{J} H = \vec{S}_1 \cdot \vec{S}_2 + \vec{S}_2 \cdot \vec{S}_3 + \epsilon (S_1^z S_2^z + S_2^z S_3^z)$$

$$= \frac{1}{2} \left\{ [\vec{S}_1 + \vec{S}_2 + \vec{S}_3]^2 - (\vec{S}_1 + \vec{S}_3)^2 - 3/4 \right\} + \epsilon (S_1^z S_2^z + S_2^z S_3^z) \tag{76}$$

$\epsilon := \Delta - 1$.

If $\epsilon = 0$ the block Hamiltonian H_B is invariant under the $SU(2)$ group and according to the introduction to this section, we should consider the tensor product decomposition:

$$\frac{1}{2} \otimes \frac{1}{2} \otimes \frac{1}{2} = \frac{1}{2} \oplus \frac{1}{2} \oplus \frac{3}{2} \tag{77}$$

The particular way of writing H_B given in Eq. (76) suggests to compose first $\vec{S}_1$ and $\vec{S}_3$ and then, the resulting spin with $\vec{S}_2$. The result of this of this compositions is given as follows:

$$|\frac{3}{2}, \frac{3}{2}\rangle = |\uparrow\uparrow\uparrow\rangle \quad E_B = J/2 \tag{78}$$

$$|\frac{3}{2}, \frac{1}{2}\rangle = \frac{1}{\sqrt{3}} (|\uparrow\downarrow\uparrow\rangle + |\downarrow\uparrow\uparrow\rangle + |\uparrow\uparrow\downarrow\rangle) \quad E_B = J/2 \tag{79}$$

$$|\frac{1}{2}, \frac{1}{2}\rangle_1 = \frac{1}{\sqrt{2}} (|\uparrow\uparrow\uparrow\rangle - |\downarrow\uparrow\uparrow\rangle) \quad E_B = 0 \tag{80}$$

$$|\frac{1}{2},\frac{1}{2}\rangle_0 = \frac{1}{\sqrt{6}}(2|\uparrow\downarrow\uparrow\rangle - |\downarrow\uparrow\uparrow\rangle - |\uparrow\uparrow\downarrow\rangle) \;\; E_B = -J \tag{81}$$

Hence for $\Delta = 0$ we could choose the spin 1/2 irrep. with basis vectors $|\frac{1}{2},\frac{1}{2}\rangle_0$ and $|\frac{1}{2},-\frac{1}{2}\rangle_0$ in order to define the intertwiner operator T_0.

However, if $\Delta \neq 0$ the states (78) -(81) are not eigenstates of (76). The full rotation group is broken down to the rotation around the z-axis. The states $|\frac{3}{2},\frac{1}{2}\rangle$ and $|\frac{1}{2},\frac{1}{2}\rangle_1$ are mixed in the new ground state which is given by:

$$|+\frac{1}{2}\rangle = \frac{1}{\sqrt{1+2x^2}}(2|\frac{1}{2},\frac{1}{2}\rangle_1 + \sqrt{2}x|\frac{3}{2},\frac{1}{2}\rangle) \tag{82}$$

where

$$x = \frac{2(\Delta-1)}{8+\Delta+3\sqrt{\Delta^2+8}} \tag{83}$$

and its energy is,

$$E_B = -\frac{J}{4}[\Delta + \sqrt{\Delta^2+8}] \tag{84}$$

along with its $|-\frac{1}{2}\rangle$ partner. This are now the two states retained in the RG method. To be more explicit, we have

$$|+\frac{1}{2}\rangle = \frac{1}{\sqrt{6(1+2x^2)}}[(2x+2)|\uparrow\downarrow\uparrow\rangle + (2x-1)|\uparrow\uparrow\downarrow\rangle + (2x-1)|\downarrow\uparrow\uparrow\rangle] \tag{85}$$

$$|-\frac{1}{2}\rangle = -\frac{1}{\sqrt{6(1+2x^2)}}[(2x+2)|\downarrow\uparrow\downarrow\rangle + (2x-1)|\downarrow\downarrow\uparrow\rangle + (2x-1)|\uparrow\downarrow\downarrow\rangle] \tag{86}$$

The intertwiner operator T_0 reads then,

$$T_0 = |+\frac{1}{2}\rangle\langle'\uparrow| + |-\frac{1}{2}\rangle\langle'\downarrow| \tag{87}$$

where $|\uparrow\rangle'$ and $|\downarrow\rangle'$ form a basis for the space $V' = \mathbf{C}^2$. The RG-equations for the spin operators $\vec{S}_i$ $(i = 1, 3)$ are then given by

$$T_0^\dagger \vec{S}_i^x T_0 = \xi^x \vec{S'}_i^x \quad i = 1, 3. \tag{88}$$

$$T_0^\dagger \vec{S}_i^y T_0 = \xi^y \vec{S'}_i^y \quad i = 1, 3. \tag{89}$$

$$T_0^\dagger \vec{S}_i^z T_0 = \xi^z \vec{S'}_i^z \quad i = 1, 3. \tag{90}$$

where ξ^x, etc are the renormalization factors which depend upon the anisotropy parameter by,

$$\xi^x = \xi^y := \frac{2(1+x)(1-2x)}{3(1+2x^2)} \tag{91}$$

$$\xi^z := \frac{2(1+x)^2}{3(1+2x^2)} \tag{92}$$

Observe the symmetry between the sites $i = 1$ and 3 which is a consequence of the even parity of the states (85) -(86).

The renormalized Hamiltonian can be easily obtained using Eqs.(88)-(92) and (74), and apart from and additive constant it has the same form as H, namely,

$$T_0^\dagger H_N(J, \Delta) T_0 = \frac{N}{3} e_B(J, \Delta) + H_{N/3}(J', \Delta') \tag{93}$$

where

$$J' = (\xi^x)^2 J \tag{94}$$

$$\Delta' = (\frac{\xi^z}{\xi^x})^2 \Delta \tag{95}$$

Iterating these equations we generate a family of Hamiltonians $H^{(m)}_{N/3^m}(J^(m), \Delta^{(m)})$. The energy density of the ground state of H_N in the limit $N \to \infty$ is then given by,

$$\lim_{N\to\infty} \frac{E_0}{N} = e_\infty^{BRG} = \sum_{m=0}^{\infty} \frac{1}{3^{m+1}} e_B(J^{(m)}, \Delta^{(m)}) \tag{96}$$

where initially $J^{(0)} = J$, $\Delta^{(0)} = \Delta$ and Eqs.(94) -(95) provide the flow of the coupling constants.

The analysis of Eq.(95) shows that there are 3 fixed points corresponding to the values $\Delta = 0$ (isotropic XX-model), $\Delta = 1$ (isotropic Heisenberg model) and $\Delta = \infty$ (Ising model). The properties of these fixed points are given in Table 6.

The computation of e_∞^{BRG} in this case is facilitated by the fact that (96) becomes a geometric series at the fixed point. The exact results concerning the models $\Delta = 0$ and $\Delta = 1$ are extracted from references [28] and [29]. The case with $\Delta \to \infty$ is exact because the states $|\pm\frac{1}{2}\rangle$ given in (85) - (86) tend in that limit to the exact ground state $|\uparrow\downarrow\uparrow\rangle$ and $|\downarrow\uparrow\downarrow\rangle$ of the Ising model. As a matter of fact,

$$|+\frac{1}{2}\rangle \simeq_{\Delta\to\infty} |\uparrow\downarrow\uparrow\rangle - \frac{1}{\Delta}|\uparrow\uparrow\downarrow\rangle - \frac{1}{\Delta}|\downarrow\uparrow\uparrow\rangle$$

$$|-\frac{1}{2}\rangle \simeq_{\Delta\to\infty} -|\downarrow\uparrow\downarrow\rangle - \frac{1}{\Delta}|\downarrow\downarrow\uparrow\rangle - \frac{1}{\Delta}|\uparrow\downarrow\downarrow\rangle$$

The region $0 < \Delta < 1$ which flows under the RG-transformation to the XX-model is massless since both $J^{(m)}$ and $\Delta^{(m)}$ go to zero. We showed at the begining of this section that all this region is critical (a line of fixed points) and therefore massless. The RG-equations (94) -(95) are not able to detect this criticality except at the point $\Delta = 0$. Only the masslessness property is detected.

The region $\Delta > 1$ which flows to the Ising model is massive and this follows from the fact that the product $J^{(m)}\Delta^{(m)}$ goes in the limit $m \to \infty$ to a constant quantity $J^{(\infty)}\Delta^{(\infty)}$ which can be computed from Eqs. (94) -(95) and (87),

$$J^{(\infty)}\Delta^{(\infty)} = \prod_{m=0}^{\infty} \frac{4}{9}\frac{(1+x_m)^4}{(1+2x_m^2)^2} \tag{97}$$

where x_m is given by (83) with Δ replaced $\Delta^{(m)}$. This quantity gives essentially the mass gap above the ground state and also the end-to-end or LRO order (Long Range Order) given by the expectation value $|\langle\vec{S}(1)\cdot\vec{S}(N)\rangle|$ in the limit $N \to \infty$.

In summary, the properties of the Heisenberg-Ising model are qualitatively and quantitatively well described in the massive region $\Delta > 1$ while in the massless region $0 < \Delta < 1$ one predicts the massless spectrum *but no criticality at each value of* Δ. This latter fact is rather subtle and elusive. One would like to construct a RG-formalism such that the Hamiltonian $H_N(\Delta)$ would be a fixed point Hamiltonian for every value of Δ in the range from -1 to 1.

The phase transition between the two regimes is correctly predicted to happen at the value $\Delta = 1$. This is a consequence of the rotational symmetry, namely at $\Delta = 1$ the system is $SU(2)$ invariant and the RG transformation has been defined as to preserve this symmetry. When $\Delta \neq 1$ the $SU(2)$ symmetry is broken and this is reflected later on in the RG-flow of the coupling constant Δ.

IX. RG FOR HEISENBERG SPIN LADDERS

Much of the El Escorial Summer School has been devoted to the nowdays very active field known as ladders systems (spin, t-J, Hubbard ...), see [32], [33], [2]. What does the BRG method have to say on these systems? We again emphasize that this is a technically simple method which produces qualitative correct results when properly applied. Later it is possible to look for numerical accuracy using DMRG, second order RG (see appendix) or some other means.

The Hamiltonian of a Heisenberg spin ladder with n_l legs, each of length N is given by,

$$\begin{aligned} \mathcal{H}_{ladder} &= \mathcal{H}_{leg} + \mathcal{H}_{rung} \\ \mathcal{H}_{leg} &= \sum_{a=1}^{n_l} \sum_{n=1}^{N} J \mathbf{S}_a(n) \cdot \mathbf{S}_a(n+1) \\ \mathcal{H}_{rung} &= \sum_{a=1}^{n_l-1} \sum_{n=1}^{N} J' \, \mathbf{S}_a(n) \cdot \mathbf{S}_a(n+1) \end{aligned} \tag{98}$$

where $\mathbf{S}_a(n)$ are spin-1/2 matrices acting on the a-th leg at the position $n = 1, \ldots, N$, and J is the intraleg coupling constant while J' is the interleg exchange coupling constants, both beign positive to guarantee AF spin ladders.

We shall concentrate on the uniform Heisenberg ladders with no staggering. There are many examples that can be worked out but to be concrete we shall pick up the 3-leg ladder system [30]. In advance, what we are going to obtain is the RG-flow towards the strong coupling limit of spin ladders. This is an alternative to the determination of the RG-fow using bosonization as performed by H.J. Schulz [31], [32]. To apply the BRG we need to set up what is the block Hamiltonian H_B which we do by forming blocks of 3 sites each along

every leg and located one block on top of another as in fig.7 In this fashion we are selecting a subset of couplings from the whole spin ladder Hamiltonian in (98). The remaining terms involving links with neighbouring blocks make up for the interblock Hamiltonian H_{BB}. We shall not write down explicitely the analytical expressions for H_B and H_{BB} as it is quite clear what is meant simply by looking at fig.7.

Now it is aparent that the standard results of the previous section are at work for spin ladders. Notice that H_B is made up of small block Hamiltonians of 3 sites as in (76) whose eigenstates and energies are already computed in (78)-(81). The renormalization process goes through all the way by truncating the block states to the lowest eigenstates, i.e., the spin doublet $|\frac{1}{2}, \pm\frac{1}{2}\rangle_0$, with energy $e_0 = -J$. In this case the embedding operator $T^{(\alpha)}$ for each block is nothing but the projector $P_0^{(\alpha)}$ onto these states; denoting

$$P_B = \prod_{\alpha=1}^{N/3} P_0^{(\alpha)} \tag{99}$$

then, to first order in J the renormalized or effective Hamiltonian acting on the states left out after the truncation is simply,

$$H_{\text{eff}} = P_B(H_B + H_{BB})P_B \tag{100}$$

Using the embedding operator (87) we arrive at,

$$P_B H_B P_B = +\frac{N}{3} e_0 = -\frac{N}{3} J \tag{101}$$

In this case the renormalization of the block Hamiltonian gives the identity because the two states retained within each block are degenerate by rotational invariance. The renormalization of the interblock Hamiltonian is also simple if we observe that H_{BB} contains products of spin operators belonging to different blocks, say $\mathbf{S}_i^\alpha \cdot \mathbf{S}_j^\beta$ where $\alpha \neq \beta$ denote neighbouring blocks and $i, j = 1, 2, 3$ are the intrablock labels used in Eq. (98). Then, according to Eq. (99) we have,

$$P_B \mathbf{S}_i^\alpha \cdot \mathbf{S}_j^\beta P_B = P_B(P_0^{(\alpha)} \mathbf{S}_i^\alpha P_0^{(\alpha)})(P_0^{(\beta)} \mathbf{S}_i^\beta P_0^{(\beta)}) P_B \tag{102}$$

Hence we only need to know how the spin operators renormalize within each block onto the new spin operators. By symmetry arguments, the renormalization spin factor denoted by ξ_i must be the same for the 3 components of the spin operators, i.e.,

$$(P_0^{(\alpha)} \mathbf{S}_i^\alpha P_0^{(\alpha)}) = \xi_i \mathbf{S}'_\alpha \tag{103}$$

where $\mathbf{S}'_\alpha$ denotes the spin 1/2 operator acting on the effective spin 1/2 subspace of the α^{th}-block. The renormalization spin factors are known from (91)-(92) to be given by,

$$\begin{aligned} \xi_1 = \xi_3 &= \frac{2}{3} \\ \xi_2 &= -\frac{1}{3} \end{aligned} \tag{104}$$

Now we are ready to compute the renormalization of the interblock Hamiltonian H_{BB}. According to Eqs. (102) and (103), the renormalization of the horizontal couplings between blocks of H_{BB} (see Fig. 7) is given by,

$$J\ \mathbf{S}_3^{(\alpha)} \cdot \mathbf{S}_1^{(\beta)} \longrightarrow J\ \xi_1 \xi_3\ \mathbf{S}_a(n') \mathbf{S}_a(n'+1) = \frac{4}{9} J\ \mathbf{S}_a(n') \mathbf{S}_a(n'+1) \tag{105}$$

while the 3 vertical couplings between two blocks are renormalized to

$$\begin{aligned} J' \left(\mathbf{S}_1^{(\alpha)} \cdot \mathbf{S}_1^{(\beta)} + \mathbf{S}_2^{(\alpha)} \cdot \mathbf{S}_2^{(\beta)} + \mathbf{S}_3^{(\alpha)} \cdot \mathbf{S}_3^{(\beta)}\right) &\longrightarrow J' \left(\xi_1^2 + \xi_2^2 + \xi_3^2\right) \mathbf{S}^{(\alpha)} \cdot \mathbf{S}^{(\beta)} \\ &= J' \mathbf{S}_a(n') \cdot \mathbf{S}_{a+1}(n'+1) \end{aligned} \tag{106}$$

We have then obtained that the renormalized Hamiltonian (100), apart from the constant term (101), is the as the original ladder Hamiltonian, but with length $N/3$ and the following renormalization of the coupling constants,

$$\begin{aligned} J &\longrightarrow \frac{4}{9} J \\ J' &\longrightarrow J' \end{aligned} \tag{107}$$

Hence the ratio J'/J increases as,

$$\frac{J'}{J} \longrightarrow \frac{9}{4} \frac{J'}{J} \tag{108}$$

after each step of the RG showing that $J'/J = \infty$ is a stable fixed point which controls the behaviour for all values of J and J', while $J'/J = 0$ is an unstable fixed point. Had we chosen blocks made up of more than 3 sites we would have obtained essentially the same result. The RG method for the simple spin chain (i.e. $n_l = 1$) where first obtained in reference [20]. According to Eq. (107) if we start in the weak coupling regime $J'/J \ll 1$, after sufficient iterations of the RG we would get an effective Hamiltonian in the strong coupling regime where we can apply the arguments of section II to derive the nature of the low lying spectrum of the theory.

X. REAL-SPACE RG APPROACH TO THE QUANTUM 2D-AF HEISENBERG MODEL

In this section we present a real-space RG treatment of the quantum two-dimensional Heisenberg antiferromagnetic model with arbitrary spin S. Most of the work using real-space RG methods has been devoted to one-dimensional problems. This is very useful because it is crucial to have an aproximate method which gives good results for both 1D and 2D problems, for it is known that mean field theory methods fail in low dimensional problems. In this regard we have recently shown that the use of quantum groups in combination of real-space methods in 1D captures the essential features exhibited by the exact solutions of models such as Heisenberg and ITF [15], [16]. Nevertheless, the main reason which has prevented the applications of the real-space RG in 2D quantum lattice Hamiltonians is the rapid growth of the number of states to be kept in a reasonable scheme of truncation of states in dimensions higher than one.

We shall be using the Block RG method in our study of the 2D Heisenberg model. This version of the RG method is suitable to achieve fully analytical treatments of interacting many-body problems. The reason for searching for complete analytical approaches as opposed to purely numerical studies relies on the necessity of having a qualitative understanding of the mechanisms responsible for the different behaviors exhibited by the Heisenberg

model itself and for its connections to more complicated related Hamiltonians such as t-J and Hubbard where the understanding of the doping effects is a big issue at stake. In order for there to be a completely analytical RG treatment in 2D we need a juidicious choice of the states to be kept as we shall see [34].

Despite of some initial controversies there is by now sufficient theoretical and experimental evidence for the existence of antiferromagnetic long range order (AF LRO) in the 2d spin 1/2 Heisenberg antiferromagnet [35] (and references therein). This property has been observed in parent compounds of hight-T_c materials such as La_2CuO_4 [35]. From a theoretical point of view this means that the strong quantum fluctuations implied by the low dimensionality and low spin do not destroy completely the Neel order, as it happens [36] in 1d. Though there is no a satisfactory physical explanation of this fact, which may be important regarding the interplay between antiferromagnetism and superconductivity upon doping. The RVB scenario originally proposed by Anderson [37,38], while yielding an appealing picture of the ground state, does not explain the presence of AF LRO. This type of order may however be incorporated a posteriori in long range RVB ansatzs of factorized form [39], with predictions similar to the ones obtained using Quantum Monte Carlo methods [40] and variational plus Lanczos techniques [41]. A class of physical systems where the RVB approach may be actually realized is in spin ladders with an even number of chains [42,43]. The previous works leave still room to investigate in more depth the interplay between the RVB scenario, or more generally "valence bond scenarios", and the AF order present in the 2d AF-magnets, described by the AF Hamiltonian $H = J \sum_{\langle i,j \rangle} \mathbf{S}_i \cdot \mathbf{S}_j$.

We have proposed a new scenario where the valence bonds, instead of resonating as in the RVB scenario, rotate around their ends under the influence of the AF background. To test this idea we propose a variational ground state in which the bonds rotate but do not resonate among themselves. We shall start by considering how the quantum fluctuations affect the classical Neel state. This is also the starting point of the spin wave theory (SW), which we would like to use for comparison of our theory. An important ingredient of our construction is the use of real-space RG techniques, which allows us to obtain exact analytical results for

any value of the spin S of the model (S is integer or half-integer and in the discussion above S=1/2.) The advantage of using a real-space RG method is that one can treat in an exact manner the local quantum fluctuations of the classical Neel state. By this we mean that if we divide the square lattice into blocks of 5 sites each, as in Figs. 8,9 and 10, then the Heisenberg Hamiltonian restricted to the blocks can be solved exactly. The ground state for every block is a spin 3/2 irrep. (if S=1/2) which is obtained by forming a singlet (bond) between the spin at the center and the ones surrounding the center (Fig. 8) According to the RG method, the spin 3/2 can be chosen as an effective spin for the renormalized lattice which now has N/5 sites. We shall show later on that the interaction between those effective spins 3/2 (or 3S more generally) is also governed by an AF-Heisenberg model with a renormalized coupling constant. Hence the RG procedure can be iterated yielding a series of effective spins which ultimately goes to its classical value, i.e. infinity! ($S \rightarrow 3S \rightarrow 3^2S \rightarrow \infty$.) We thus obtain in an economical and simple way the important result that the 2D AF-Heisenberg models belongs to the universality class of the 2D classical Heisenberg model. For a sigma model derivation of this result see ref. [45]. The rotating bond picture puts in correspondence various approaches to the 2D AF-Heisenberg model.

Let us begin our approach by considering the cluster of 5 spins 1/2 of Fig.8 a). The configuration showed in Fig.8 a) is the exact ground state of the Ising piece of the Heisenberg Hamiltonian, given by $H_z = J \sum_{i=1,...,4} S_0^z S_i^z$, where S_0^z and S_i^z are the third component of the spin operators at the center and the i^{th} position off the center respectively. As soon as the "transverse" Hamiltonian $H_{xy} = J \sum_{i=1,...,4} (S_0^x S_i^x + S_0^y S_i^y)$ is switched on, the down-spin in the middle starts to move around the cluster, and a valence bond between the center and the remaining sites is formed in a s-wave ($l = 0$) symmetric state as shown in Fig.8 b). Other rotational states with $l \neq 0$ may appear corresponding to excitations (l being the orbital angula momentum of the bond). An alternative description of this state is given by first combining the 4 spins sourrounding the center into a spin 2 irrep, which in turn is combined with the spin 1/2 at the center yielding a spin 3/2 irrep with energy $e_0 = -3J/2$. If instead of the spin 1/2 at each site there is a spin S the previous analysis can be easily generalized

as follows: the ground state of the AFH Hamiltonian of the 5-cluster has total spin 3S and is obtained by first combining all the surrounding spins into a spin 4S, which in turn becomes a spin 3S after multiplication with the spin S at the center. In a certain sense this state can be viewed as the formation of bonds between the center and its four neighbours. After applying several steps of the real-space RG, as we shall see below, new bonds are generated between sites at longer distances apart. Thus our valence-bond scenario is a type of long range valence bond state.

To study the AFH model in the entire square lattice we begin by first tesselating this plane using the cluster of Fig.8 as the fundamental cell (see Fig. 9). Notice that the centers of the 5-cluster form a new square lattice with lattice spacing $a' = \sqrt{5}a$. Given this tesselation we can apply the standard RG method of replacing clusters of spins by an effective spin [13,14]. This method has been applied for the 1d AFH model by Rabin [20] for clusters or blocks with 3 sites, obtaining a ground state energy with an error of 12%. The effective spin of every 3-block in 1d has spin 1/2. In our case, as we have discussed above, the effective spin of the 5-blocks have spin 3S and the energy per block equal to $e_0 = -JS(4S+1)$. The effective spins $S' = 3S$ interact by means of an effective Hamitonian which to first order in perturbation theory can be derived if we know the renormalization of the spin operators $\mathbf{S}_\alpha \to \xi_\alpha \mathbf{S}', \alpha = 0, 1, \ldots, 4$.

The *renormalization spin factor* ξ_α can be shown to be given by the sum $\xi_\alpha = \frac{1}{3S} \sum_{m_0,m_1,\ldots,m_4} m_\alpha (C^{3S}_{m_0,m_1,\ldots,m_4})^2$ subject to the constraint $\sum_{\alpha=0}^4 m_\alpha = 3S$. $C^{3S}_{m_0,m_1,\ldots}$ is the CG coefficient which describes the ground state of spin 3S in terms of the 5 original spins S, whose expression is a product of 4 standard CG coefficients. The ξ_α satisfy the *sum rule* $\sum_{\alpha=0}^4 \xi_\alpha = 1$. We arrive at the following result,

$$\xi_\alpha(S) = \frac{1}{3S}\frac{6S+1}{8S+1}\frac{[(2S)!]^5}{[(8S)!]^2} \times \sum_{m_1,\ldots,m_4} m_\alpha \frac{(4S-\sum_1^4 m_i)!\ [(4S+\sum_1^4 m_i)!]^2}{\prod_1^4 (S-m_i)!\ (S+m_i)!\ [-2S+\sum_1^4 m_i]!} \tag{109}$$

where if $\alpha = 0$ then $m_0 = 3S - \sum_1^4 m_i$. It follows that the renormalization factors for the four external spins in the 5-block are all equal $\xi_1 = \xi_2 = \xi_3 = \xi_4 \equiv \xi(S)$, while that of

the central spin ξ_0 is determined by the sum rule. Amazingly enough the sum (109) can be performed in a close manner yielding,

$$\xi(S) = \frac{1}{3}\,\frac{S+\frac{1}{4}}{S+\frac{1}{3}} \tag{110}$$

For spin $S = \frac{1}{2}$ one obtains $\xi(\frac{1}{2}) = \frac{3}{10}$. Moreover, Eq. (110) correctly reproduces the classical limit $\lim_{S\to\infty}\xi(S) = \frac{1}{3}$ (recall $S = S^{\rm old} = \frac{1}{3}S' = \xi_{\rm cl}S'$). Notice also that the value for $S = \frac{1}{2}$ is already close to the classical value.

The RG-equations for the spin operators $\mathbf{S_i}$ $i = 1, 2, 3, 4$ allows us to compute the renormalized Hamiltonian H' which turns out to be of the same form as the original AFH Hamiltonian. In fact, we arrive at the following RG-equations,

$$\begin{aligned} H'(N,S,J) &= -JS(4S+1)\frac{N}{5} \\ &\quad + H(\tfrac{N}{5}, 3S, 3\xi^2(S)J) \end{aligned} \tag{111a}$$

$$N' = \frac{N}{5},\ S' = 3S,\ J' = 3\xi^2(S)J \tag{111b}$$

where the first contribution in Eq. (111a) comes from the energy of the blocks. As $3\xi^2(S) < 1$, the flow equation (111b) implies that the coupling constant flows to zero $J^{(n)} \overset{n\to\infty}{\to} 0$ which means that the AFH model remains *massless* for arbitrary value of the spin S. This fact allows us to compute the density of energy $e_\infty(S)$ (per site) as the following series,

$$e_\infty(S) = -\tfrac{1}{5}\sum_{n=0}^{\infty}\tfrac{1}{5^n}J^{(n)}S^{(n)}(4\times 3^n S + 1) \tag{112a}$$

$$S^{(n+1)} = 3S^{(n)},\ J^{(n+1)} = 3\xi^2(S^{(n)})J^{(n)} \tag{112b}$$

Using eqs. (112a) and (112b) we can compute the ground state energy of our variational RG state for any value of the spin S. In particular for S=1/2 we get the value e_∞ = -0.5464. This value has to be compared with the "exact" numerical result -0.6692, which is obtained using Green-function Monte Carlo methods [40], and the spin wave value which is -0.6703. The difference between our result and the Green Function MC or SW is quite big and around

0.12. To clarify the origin of this departure we have considered the semiclassical expansion of Eq. (112a) and compare it with the standard formula of Anderson and Kubo [49],

$$e_\infty^{RG} = -2S(S + \frac{0.0223}{S} + \cdots) \tag{113a}$$

$$e_\infty^{sw} = -2S(S + 0.158 + \frac{0.0062}{S} + \cdots) \tag{113b}$$

The important observation is that the term linear in S is absent in our formula (113a). The reason for this is that we are using a first order RG method for which the ground state energy follows from the formula $E_{\rm GS} = \langle\Psi_0|H|\Psi_0\rangle$, where $|\Psi_0\rangle$ is the variational ground state constructed by the RG method. Now it is easy to see that taking $|\Psi_0\rangle$ to be simply the Neel state one has to go to second order perturbation theory (PT) to get a linear term in S, which turns out to be given by $S/4 + 1/32 + O(1/S)$. It is clear that the "missing energy " 0.12 is due to this peculiarity of the first order PT. To remedy this one should implement the RG method with second order PT. In 1D and for S=1/2 this can be done, obtaining for the ground state energy density $e_\infty = -0.4530$ which is comparable in precision with the spin wave result -0.4647 (recall that the exact value is -0.4431.) The latter computation in 2D is much more involved but it is expected to yield a result close to the spin wave result.

In order to have a better insight into the physics of the model it is convenient to compute the staggered magnetization $M \equiv \langle\frac{1}{N}\sum_j(-1)^j S_j^z\rangle$. We have been able to obtain a closed formula for arbitrary spin S which is capable of analytical study. To this purpose, we use the RG-equality for V.E.V. $\langle\psi_0|\mathcal{O}|\psi_0\rangle = \langle\psi_0'|\mathcal{O}'|\psi_0'\rangle$ for renormalized observables $\mathcal{O}'$ in the ground state and divide the sum in M into 5-block contributions. With the help of the renormalization spin factors we arrive at the RG-equation for the staggered magnetization,

$$M_N(S) = \frac{8\xi(S) - 1}{5} M_{N/5}(3S) \tag{114}$$

The explicit knowledge of $\xi(S)$ (109) allows us to solve this RG-equation for the staggered magnetization in the thermodynamic limit $N \to \infty$. In fact, as we know by now that the Hamiltonian renormalizes to its classical limit, we have $\lim_{S\to\infty} M(S) = S$. Defining

$M(S) \equiv Sf(S)$, Eq. (114) amounts to solving the equation $f(S) = \frac{S+1/5}{S+1/3} f(3S)$ subject to the boundary condition $f(\infty) = 1$. Thus, we obtain the following formula for the staggered magnetization for arbitrary spin,

$$M(S) = S \prod_{n=0}^{\infty} \frac{S + \frac{1}{5}3^{-n}}{S + \frac{1}{3}3^{-n}} \tag{115}$$

This is a nice formula in several regards. For spin $S = \frac{1}{2}$ we get $M(\frac{1}{2}) = 0.373$ to be compared with the most accurate Quantum Monte Carlo reslult [46] which is 0.3074 (earlier numerical results were obtained with Green function QMC methods [40] and Variational Monte Carlo plus Lanczos algorithm [41]). Other approximate methods employed so far lead to values of $M(\frac{1}{2})$ such as, e.g., spin wave theory plus $1/S$-expansion to order S^{-2} gives [47,48] 0.3069 (earlier SW results were provided by Anderson and Kubo [49]), spin wave theory plus perturbation theory gives [50] 0.313, etc. Our value is close to the one found [51] with pertubation theory around the Ising model to order 4 which is 0.371. We can equally get values of the staggered magnetization for arbitrary spin. For spin S=1, our formula (115) gives 0.8454 to be compared with 0.8043 using SW to order [47] $1/S^2$ and 0.8039 obtained by Wheihong et al. [52] using series expansions.

Another interesting feature of our formula (115) is that it allows us to make a $1/S$-expansion yielding the result,

$$M_{\infty}^{\mathrm{RG}}(S) = S - 0.2 + 0.06\frac{1}{S} + O(1/S^2) \tag{116a}$$

$$M_{\infty}^{sw}(S) = S - 0.198 + O(1/S^2) \tag{116b}$$

Observe the excellent agreement between the order S^0 term in both formulas. Recall that equation (116a) is derived using first order PT. We expect that a second order RG would further lower the value of $M(S)$, in agreement with the numerical result.

In summary we can claim that the rotating-valence-bond scenario gives a consistent and suggestive picture of the ground state of the 2D AF-Heisenberg model: the quantum fluctuations of the Neel state consist of rotating bonds which appear at all scales corresponding to effective spins which renormalize towards the classical value.

XI. APPENDIX: SECOND ORDER FORMALISM FOR THE STANDARD BRG METHOD

The modern fashion to include correlations between blocks in the real-space RG is the DMRG [1]. Nevertheless, there is an old way to include those correlations which we believ has been overlooked in the past. It amounts to include a second order contribution to the BRG. Recall that the standard BRG in previous sections is a first order method from the point of view of Perturbation Theory (P.T.), i.e., the interblock Hamiltonian H_{BB} is treated perturbatively in first order. We can extend this treatment [30] to second order P.T. in the usual fashion and thus arrive to an effective Hamiltonian given by:

$$H_{eff} = P_B[H_B + H_{BB} + H_{BB}(1-P_B)\frac{1}{E_B - H_B}(1-P_B)H_{BB}]P_B \tag{117}$$

where E_B is the ground state energy of the block and P_B denotes the projector onto te ground state of the block. This is nothing but the intertwiner operator of section 2.

As a matter of illustration, we shall work out this formalism for the isotropic AF Heisenberg model in 1D using the 3-site block BRG explained in section 8. Moreover, we restrict to spin 1/2. Denote each block with an index α. Thus, the Hilbert space for each block $\mathcal{H}^\alpha$ is decomposed into 1/2, 1/2 and 3/2-spin subspaces,

$$\mathcal{H}^{(\alpha)} = \mathcal{H}_0^{(\alpha)}(1/2) \oplus \mathcal{H}_1^{(\alpha)}(1/2) \oplus \mathcal{H}_2^{(\alpha)}(3/2) \tag{118}$$

Correspondingly, we introduce 3 projectors onto those subspaces,

$$P_0^{(\alpha)} + P_1^{(\alpha)} + P_2^{(\alpha)} = \mathbf{1}^{(\alpha)} \tag{119}$$

They satisfy the following properties that we will be useful,

$$P_B = \prod_{\alpha=1}^{N'} P_0^{(\alpha)} \tag{120a}$$

$$1 - P_B = 1 - \prod_{\alpha=1}^{N'} P_0^{(\alpha)} \neq \prod_{\alpha=1}^{N'} (1 - P_0^{(\alpha)}) \tag{120b}$$

$$(P_m^{(\alpha)})^2 = P_m^{(\alpha)}, \quad P_m^{(\alpha)} P_{m'}^{(\alpha)} = 0, \quad m \neq m' \tag{120c}$$

$$P_m^{(\alpha)} P_{m'}^{(\beta)} = P_{m'}^{(\beta)} P_m^{(\alpha)} \tag{120d}$$

where $N' = N/3$ and m indicates the site in each block.

With the help of these properties, the second order contribution to H_{eff} in (117), denoted by $H_{eff}^{(2)}$, can be given the following form containing 3 types of terms:

$$\begin{aligned} H_{eff}^{(2)} = P_B \sum_{\alpha=1}^{N'} \sum_{m_\alpha \neq 0} \frac{1}{e_0 - e_{m_\alpha}} \\ \{[(P_0^{(\alpha-1)} \mathbf{S}_3^{(\alpha-1)} P_0^{(\alpha-1)}) \cdot (P_0^{(\alpha)} \mathbf{S}_1^{(\alpha)} P_{m_\alpha}^{(\alpha)})][(P_{m_\alpha}^{(\alpha)} \mathbf{S}_3^{(\alpha)} P_0^{(\alpha)}) \cdot (P_0^{(\alpha+1)} \mathbf{S}_1^{(\alpha+1)} P_0^{(\alpha+1)}) \\ + [(P_0^{(\alpha)} \mathbf{S}_3^{(\alpha)} P_{m_\alpha}^{(\alpha)}) \cdot (P_0^{(\alpha+1)} \mathbf{S}_1^{(\alpha+1)} P_0^{(\alpha+1)})][(P_0^{(\alpha-1)} \mathbf{S}_3^{(\alpha-1)} P_0^{(\alpha-1)}) \cdot (P_{m_\alpha}^{(\alpha)} \mathbf{S}_3^{(\alpha)} P_0^{(\alpha)})]\} P_B \\ + P_B \sum_{\alpha=1}^{N'} \sum_{(m_\alpha, m_{\alpha+1}) \neq (0,0)} \frac{1}{2e_0 - e_{m_\alpha} - e_{m_{\alpha+1}}} \\ [(P_0^{(\alpha)} \mathbf{S}_3^{(\alpha)} P_{m_\alpha}^{(\alpha)}) \cdot (P_0^{(\alpha+1)} \mathbf{S}_1^{(\alpha+1)} P_{m_{\alpha+1}}^{(\alpha+1)})][(P_{m_\alpha}^{(\alpha)} \mathbf{S}_3^{(\alpha)} P_0^{(\alpha)}) \cdot (P_{m_{\alpha+1}}^{(\alpha+1)} \mathbf{S}_1^{(\alpha+1)} P_0^{(\alpha+1)})] P_B \end{aligned} \tag{121}$$

In order to work out this expression (121) towards a manageable result, we need to perform a renormalization of the spin operators both in both subspaces of spin-1/2 (recall that in sect.8 we did it only for the lowest energy spin 1/2.)

Let us introduce the following notation for the 4 states of spin 1/2:

$$|m, \beta\rangle \quad \text{with} \quad m = \pm 1/2, \beta = 0, 1 \tag{122}$$

Denote by $\mathbf{S}'$ the effective spin-1/2 coming out of the block renormalization. Then,

$$\langle m, \beta | \mathbf{S}_i | m', \beta' \rangle = \langle m | \mathbf{S}' | m' \rangle (\rho_i)_{\beta, \beta'} \tag{123}$$

with the ρ-matrices given by,

$$\rho_1 = \begin{pmatrix} 2/3 & -1/\sqrt{3} \\ -1/\sqrt{3} & 0 \end{pmatrix}, \quad \rho_2 = \begin{pmatrix} -1/3 & 0 \\ 0 & 1 \end{pmatrix}, \quad \rho_3 = \begin{pmatrix} 2/3 & 1/\sqrt{3} \\ 1/\sqrt{3} & 0 \end{pmatrix} \tag{124}$$

Thus, the spin renormalization that we were searching for is summarized in

$$P_\beta \mathbf{S}_i P_{\beta'} = \mathbf{S}' (\rho_i)_{\beta, \beta'} \tag{125}$$

Namely,

$$P_0\mathbf{S}_1P_0 = P_0\mathbf{S}_3P_0 \equiv (\xi^{(0)} = \frac{2}{3})\mathbf{S}' \tag{126a}$$

$$P_0\mathbf{S}_1P_1 = P_1\mathbf{S}_1P_0 \equiv (\xi_1^{(0)} = \frac{-1}{\sqrt{3}})\mathbf{S}' \tag{126b}$$

$$P_0\mathbf{S}_3P_1 = P_1\mathbf{S}_3P_0 \equiv (\xi_3^{(0)} = \frac{1}{\sqrt{3}})\mathbf{S}' \tag{126c}$$

Upon substitution of these expressions in (121) we are led to the renormalization of the Hamiltonian:

$$H_{eff}^{(2)} = \sum_{\alpha=1}^{N'}[d^{(2)} + J_1^{(2)}\mathbf{S}_\alpha \cdot \mathbf{S}_{\alpha+1} + J_2\mathbf{S}_\alpha \cdot \mathbf{S}_{\alpha+2}] \tag{127}$$

$$H_{eff}^{(0+1)} = \sum_{\alpha=1}^{N'}[d^{(0)} + J_1^{(1)}\mathbf{S}_\alpha \cdot \mathbf{S}_{\alpha+1}] \tag{128}$$

with the following numerical values,

$$\begin{aligned} &d^{(0)} = -1, \qquad\quad J_1^{(1)} = \tfrac{4}{9} = 0.44 \\ &d^{(2)} = -0.104861,\ J_1^{(2)} = \tfrac{211}{1620} = 0.130247,\ J_2 = \tfrac{10}{243} = 0.0411523 \end{aligned} \tag{129}$$

Altogether, we end up with the following effective Hamiltonian in which the second order formalism employed shows up as a nearest-neighbour coupling J_2,

$$H_{eff} = \sum_{\alpha=1}^{N'}[d + J_1\mathbf{S}_\alpha \cdot \mathbf{S}_{\alpha+1} + J_2\mathbf{S}_\alpha \cdot \mathbf{S}_{\alpha+2}] \tag{130}$$

with,

$$d = -1.104861, \quad J_1 = 0.574691, \quad J_2 = 0.0411523 \tag{131}$$

We can now iterate this RG procedure as usual to obtain the RG-flow equations for the two coupling constants J_1 and J_2:

$$\begin{aligned} J_1^{(m+1)} &= aJ_1^{(m)} - bJ_2^{(m)} \\ J_2^{(m+1)} &= cJ_2^{(m)} \end{aligned} \tag{132}$$

$$a = 0.57491 \quad b = 0.44444 \quad c = 0.041152$$

The fixed points of these RG-eqs. are simply,

$$(\frac{J_2}{J_1})_c = \frac{1}{2}[\frac{a}{b} \pm \sqrt{(\frac{a}{b})^2 - 4(\frac{c}{b})}] \tag{133}$$

Upon iteration the system flows towards the smallest fixed point,

$$(\frac{J_2}{J_1})_c = 0.076084 \tag{134}$$

This happens to be an understimation of the numerical value.

Finally, we get a series expressing the ground state energy to second order in RG,

$$e_\infty = \sum_{m=0}^{\infty} \frac{1}{3^{m+1}}[-\gamma_1 J_1^{(m)} + \gamma_2 J_2^{(m)}] \tag{135}$$

with $\gamma_1 = -1.104861$, $\gamma_2 = 0.25$.

The above sum can be computed exactly by introducing generating functions $J_i(x) \equiv \sum_{m=0}^{\infty} x^m J_i^{(m)}$, $i = 1, 2$ and using the RG-eqs. (132),

$$J_1(x) = \frac{1}{1 - ax + bcx^2}, \quad J_2(x) = \frac{cx}{1 - ax + bcx^2} \tag{136}$$

Thus,

$$e_\infty = -\frac{1}{3}\frac{\gamma_1 - \gamma_2 \frac{c}{3}}{1 - \frac{a}{3} + \frac{bc}{9}} \tag{137}$$

and substituting the values of γ_1 and γ_2, we get

$$e_\infty^{(2RG)} = -0.453002 \tag{138}$$

This is to be compared with the exact value $e_\infty^{(exact)} = -0.4431$ which amounts to a 2.2 % error. This results improves even the spin wave result $e_\infty^{(sw)} = -S^2 - 0.36338s - 0.033011 = -0.4647$ which is a 4 % off the exact value. Recall that $e_\infty^{(1RG)} = -0.391304$ (11.6 % .)

Acknowledgements The work presented in these notes has been done in collaboration with Germán Sierra and I have enjoyed many conversations on real-space RG methods and

related topics with him. Sections on the CBRG method are also in collaboration with J. Rodriguez-Laguna. I also thank R. Shankar for many comments on renormalization group during his visit at CSIC (Madrid). I acknowledge many useful discussions with the lecturers at the El Escorial Summer School, specially Steve White, T. Nishino, A. Sandvik.
This work has been partially supported in part by CICYT under contract AEN93-0776.

REFERENCES

[1] S.R. White, *Phys. Rev. Lett.* **69**, 2863 (1992); *Phys. Rev. B* **48**, 10345 (1993).

[2] S.R. White, Proceedings of El Escorial Summer School 1996, and references therein.

[3] S.R. White, Preprint cond-mat/9604129.

[4] T. Nishino, "Density Matrix and Renormalization for Classical Lattice Models", proceedings in this volume.

[5] J. Pérez-Conde, Proceedings of El Escorial Summer School 1996, and references therein.

[6] K.R. Wilson, *Rev. Mod. Phys.* **47**, 773 (1975).

[7] P.W. Anderson, *J. Phys. C* **3**, 2436 (1970).

[8] Hirsch, J. *1983, Phys. Rev. B* **28***, 4059*, *1985, Phys. Rev. B* **31***, 4403*; Hirsch, J. and Lin, H.Q., *1988, Phys. Rev. B* **37***, 5070.*

[9] S.D. Drell, M. Weinstein, S. Yankielowicz, *Phys. Rev. D* **16**, 1769 (1977).

[10] R. Jullien, P. Pfeuty, J.N. Fields, S. Doniach, *Phys. Rev. B* **18**, 3568 (1978).

[11] Hirsch, J. *1980, Phys. Rev. B* **22***, 5259.*

[12] M.A. Martín-Delgado and G. Sierra, "Analytic Formulations of the Density Matrix Renormalization Group", Int. J. Mod. Phys. **A11** 3145, (1996).

[13] "Real-Space Renormalization", editors Burkhardt, T.W. and van Leeuwen, J.M.J., series topics in Current Physics **30**, Springer-Verlag 1982.

[14] J. González, M.A. Martín-Delgado, G. Sierra, A.H. Vozmediano,
Quantum Electron Liquids and High-T_c Superconductivity,
Lecture Notes in Physics, Monographs vol. **38**, Springer-Verlag 1995.

[15] M.A. Martín-Delgado and G. Sierra, "Real Space Renormalization Group Methods and Quantum Groups". Phys. Rev. Lett. **76**,1146 (1996).

[16] M.A. Martín-Delgado and G. Sierra, in "From Field Theory to Quantum Groups". World Scientific Publishers 1996.

[17] S.R. White, R.M. Noack, *Phys. Rev. Lett.* **68**, 3487 (1992).

[18] Wilson, K.G., *1986, unpublished informal talk.*

[19] V. Karimipour and A. Langari, "A Modified Quantum Renormalization Group for the XXZ Spin Chain", preprint 1996, private communication.

[20] J.M. Rabin, *Phys. Rev. B* **21**, 2027 (1980).

[21] M.A. Martín-Delgado and G. Sierra, "The Role of Boundary Conditions in the Real-Space Renormalization Group". Phys. Lett. **B364** 41, (1995).

[22] M.A. Martín-Delgado, J. Rodriguez-Laguna and G. Sierra, "The Correlated Block Renormalization Group". Nucl. Phys. **B473** 685, (1996).

[23] A. Fernández-Pacheco, *Phys. Rev. D* **19**, 3173 (1979).

[24] T. Nishino, "Density Matrix Renormalization Group Method for 2D Classical Models", J. Phys. Soc. Jpn. **64** (1995) 3958-3961.

[25] T. Nishino and K. Okunishi, "Corner Transfer Matrix Renormalization Group Method", J. Phys. Soc. Jpn. **65** (1996) 891-894. cond-mat/9507087.

[26] S. Ostlund and S. Rommer, "Thermodynamic limit of the density matrix renormalization for the spin-1 Hesisenberg chain". Phys. Rev. Lett. **75**, 3537 (1996).

[27] T. Nishino and K. Okunishi, "Product Wave Function Renormalization Group". J. Phys. Soc. Jpn. **64** (1995) 4084-4087. cond-mat/9510004.

[28] Lieb, E., Schultz, T. and Mattis, D. *1961, Ann. Phys.* **16***, 407*

[29] Orbach, R., *1958, Phys. Rev.* **112***, 309*

[30] M.A. Martín-Delgado and G. Sierra, unpublished work 1996.

[31] H. J. Schulz, Phys. Rev. B **34**, 6372 (1986).

[32] H.J. Schulz, Proceedings of El Escorial Summer School 1996, and references therein.

[33] G. Sierra, Proceedings of El Escorial Summer School 1996, and references therein.

[34] G. Sierra and M.A. Martín-Delgado, "Real Space Renormalization Group Approach to the 2D Antiferromagnetic Heisenberg Model", preprint (1996).

[35] E. Manousakis, Rev. Mod. Phys. **63**, 1 (1991).

[36] H.A. Bethe, Z. Phys. **71**, 205 (1931).

[37] P.W. Anderson, Science **235**, 1196 (1987).

[38] S.A. Kivelson, D.S. Rokhsar and J.P. Sethna, *Phys. Rev. B* **35**, 8865 (1987).

[39] S. Liang, B. Doucot and P.W. Anderson, *Phys. Rev. Lett.* **61**, 365 (1988).

[40] J. Carlson, *Phys. Rev. B* **40**, 846 (1989).

[41] Hebb and T. M. Rice, *Z. Phys. B* **90**, 73 (1993).

[42] S. White, R. Noack and D. Scalapino, *Phys. Rev. Lett.* **73**, 886 (1994).

[43] E. Dagotto and T.M. Rice, *Science* **271**, 618 (1996).

[44] P. Fazekas and P.W. Anderson, *Phil. Mag.* **30**, 432 (1974)

[45] S. Chakravarty, B.I. Halperin and D.R. Nelson, *Phys. Rev. Lett.* **60**, 1057 (1988).

[46] Wise and Ying, *Z. Phys. B* **93**, 147 (1994).

[47] C.J. Hamer, Z. Weihong and P. Arndt, *Phys. Rev. B* **46**, 6276 (1992).

[48] C.M. Canali and M. Vallin, *Phys. Rev. B* **48**, 3264 (1992).

[49] P.W. Anderson, *Phys. Rev. B* **6**, 694 (1952); R. Kubo, *Phys. Rev.* **87**, 568 (1952).

[50] D. Huse, *Phys. Rev. B* **37**, 2380 (1988).

[51] M. Parrinello and T. Arai, *Phys. Rev. B* **10**, 265 (1974).

[52] Z. Weihong, J. Oitmaa and C.J. Hamer, *Phys. Rev. B* **43**, 8321 (1991).

FIGURES

FIG. 1. a) Block decomposition of a square lattice into 4-site blocks. b)Squematic truncation of states in the BRG method associated to the previous lattice decomposition.

FIG. 2. a) Ground state ψ_0 and first excited state ψ_1 for the Hamiltonian H_{Fixed} with fixed BC's. b) Ground state ψ_0 and first excited state ψ_1 for the Hamiltonian H_{Free} with free BC's.

FIG. 3. Building blocks of the 3-site BRG for the tight-binding model in 1D with free BC's. a) Ground state, b) First excited estate, c) Second excited state.

FIG. 4. Pictorical decomposition of a given Hamiltonian H into uncorrelated A-operators, correlation B_L- B_R-operators and interaction C-operators according to the CBRG method. B_1 is a superblock made up of two L_1 and R_1 blocks.

FIG. 5. The n^2/N^2-law for the first 5 excited states of the 1D Tight-Binding Model for a chain of $N = 12 \times 2^m$ sites with Free-Free BC's. This is a $\ln E_n$-$\ln m$ plot.

FIG. 6. The wave function reconstruction for the first 5 excited states of the 1D Tight-Binding Model for a chain of $N = 12 \times 2^6 = 768$ sites with Free-Free BC's. We have scaled up the exact results by a factor of 1.23 for clarity.

FIG. 7. Block decomposition associated to the standard BRG method applied to the uniform 3-leg Heisenberg ladder.

FIG. 8. a) The antiferromagnetic 5-block state. b) Formation of a rotating-valence-bond state upon applying the H_{xy} part of the Hamiltonian to the AF 5-block state.

FIG. 9. Artistic tesselation of the square lattice with 5-site blocks.

FIG. 10. The two-dimensional square lattice tesselated by the 5-block. Dahed lines are nearest-neighbours in the renormalized lattice.

TABLES

Energies	Exact	CBRG	DMRG
E_0	0	1.1340×10^{-14}	1.0×10^{-6}
E_1	1.6733×10^{-5}	1.9752×10^{-5}	1.6733×10^{-5}
E_2	6.6932×10^{-5}	7.6552×10^{-5}	6.6932×10^{-5}
E_3	1.5060×10^{-4}	1.8041×10^{-5}	1.5060×10^{-4}
E_4	2.6772×10^{-4}	2.9681×10^{-4}	2.6772×10^{-4}
E_5	4.1831×10^{-4}	5.1078×10^{-4}	4.1831×10^{-4}

TABLE I. Exact and CBRG Values of Low Lying States for the 1D Tight-Binding Model for a chain of $N = 12 \times 2^6 = 768$ sites with Free-Free BC's. DMRG values are also given.

m	N=12 2^m	$E_1^{(exact)}(N)$	$E_1^{(CBRG)}(N)$	$E_1^{(DMRG)}(N)$
0	12	6.8148×10^{-2}	6.8148×10^{-2}	6.8148×10^{-2}
1	24	1.7110×10^{-2}	1.7375×10^{-2}	1.7110×10^{-2}
2	48	4.2826×10^{-3}	4.4694×10^{-3}	4.2826×10^{-3}
3	96	1.0708×10^{-3}	1.1515×10^{-3}	1.0708×10^{-3}
4	192	2.6772×10^{-4}	2.9681×10^{-4}	2.6772×10^{-4}
5	384	6.6932×10^{-5}	7.6552×10^{-5}	6.6932×10^{-5}
6	768	1.6733×10^{-5}	1.9752×10^{-5}	1.6733×10^{-5}
	$\gg 1$	π^2/N^2	$9.8080/N^2$	$9.8696/N^2$

TABLE II. Exact and new CBRG values of the first excited state for the 1D Tight-Binding Model with Free-Free BC's. DMRG values are also given.

Energies	Exact	Standard BRG	CBRG
E_0	1.7754×10^{-5}	1.5771×10^{-2}	1.8409×10^{-5}
E_1	1.5043×10^{-4}	4.2679×10^{-2}	1.6655×10^{-4}
E_2	4.1761×10^{-4}	4.2794×10^{-2}	4.6408×10^{-4}
E_3	8.1831×10^{-4}	4.3053×10^{-2}	9.1450×10^{-4}
E_4	1.3520×10^{-3}	4.3173×10^{-2}	1.5179×10^{-3}
E_5	2.0196×10^{-3}	4.4288×10^{-2}	2.2852×10^{-3}

TABLE III. Exact, Standard RG and CBRG Values of Low Lying States for the 1D Tight-Binding Model for a chain of $N = 12 \times 2^5 = 384$ sites with Free-Fixed BC's.

Energies	Exact	Standard BRG	CBRG	DMRG
E_0	6.6585×10^{-5}	5.8116×10^{-2}	7.0843×10^{-5}	6.7×10^{-5}
E_1	2.6633×10^{-4}	5.8155×10^{-2}	2.9403×10^{-4}	2.66×10^{-4}
E_2	5.9924×10^{-4}	5.8268×10^{-2}	6.3690×10^{-4}	5.99×10^{-4}
E_3	1.0653×10^{-3}	5.8470×10^{-2}	1.2289×10^{-3}	1.065×10^{-3}
E_4	1.6644×10^{-3}	5.8717×10^{-2}	1.7707×10^{-3}	1.664×10^{-3}
E_5	2.3966×10^{-3}	5.9106×10^{-2}	2.7311×10^{-3}	2.397×10^{-3}

TABLE IV. Exact, Standard RG and CBRG Values of Low Lying States for the 1D Tight-Binding Model for a chain of $N = 12 \times 2^5 = 384$ sites with Fixed-Fixed BC's. DMRG values are also given.

Energies	Exact	CBRG
E_0	0	9.6114×10^{-35}
E_1	1.5056×10^{-4}	1.9390×10^{-4}
E_2	1.5056×10^{-4}	1.9390×10^{-4}
E_3	3.0012×10^{-4}	3.8781×10^{-4}

TABLE V. Exact and CBRG Values of Low Lying States for the 2D Tight-Binding Model for a lattice of $N = 4 \times 4 \times 4^6 = 65536$ sites with Free BC's.

TABLE VI. Fixed Points of the Anisotropic AF-Heisenberg Model

Δ	0	1	∞
R_∞^{BRG}	-0.2828	-0.3913	$-\frac{1}{4}\Delta$
e_∞^{exact}	-0.3183	-0.4431	$-\frac{1}{4}\Delta$
$\frac{e^B - e^{exact}}{e^{exact}} \times 100$	11%	12%	0

a)

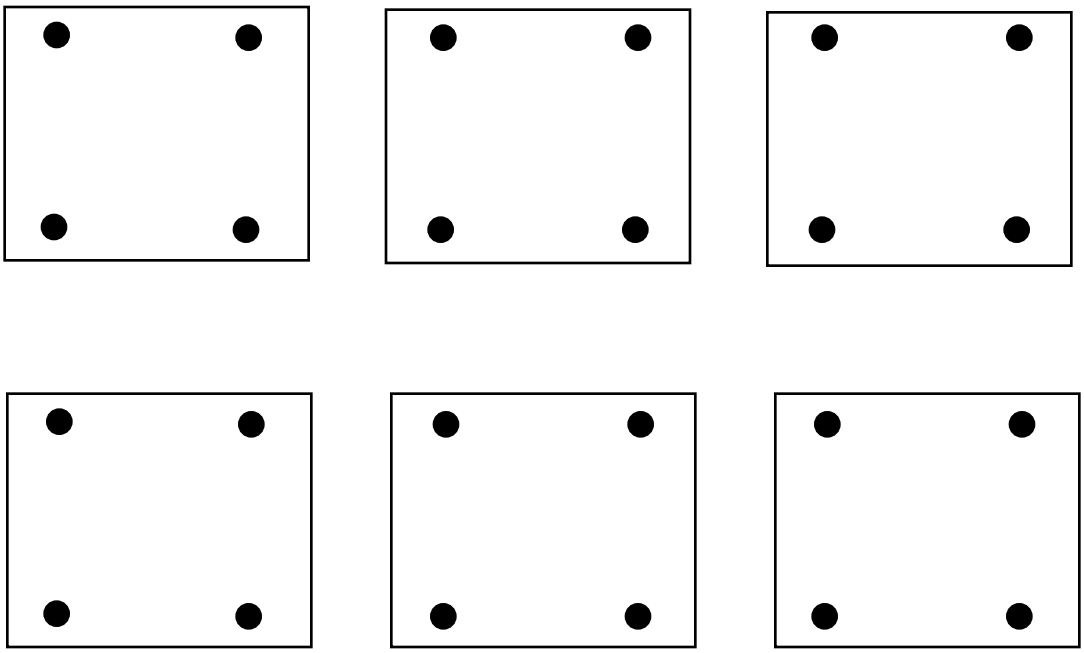

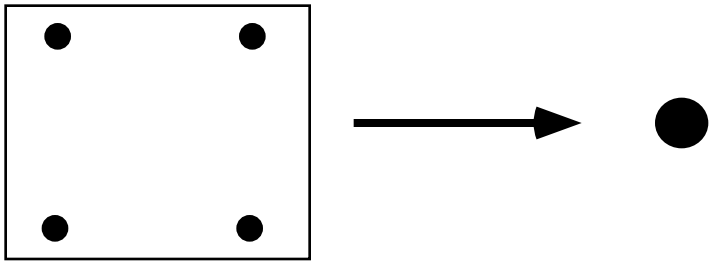

b)

Figure 1

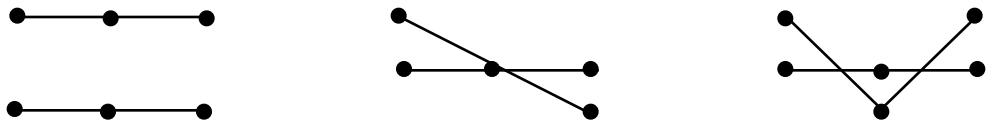

a) b) c)

Figure 3

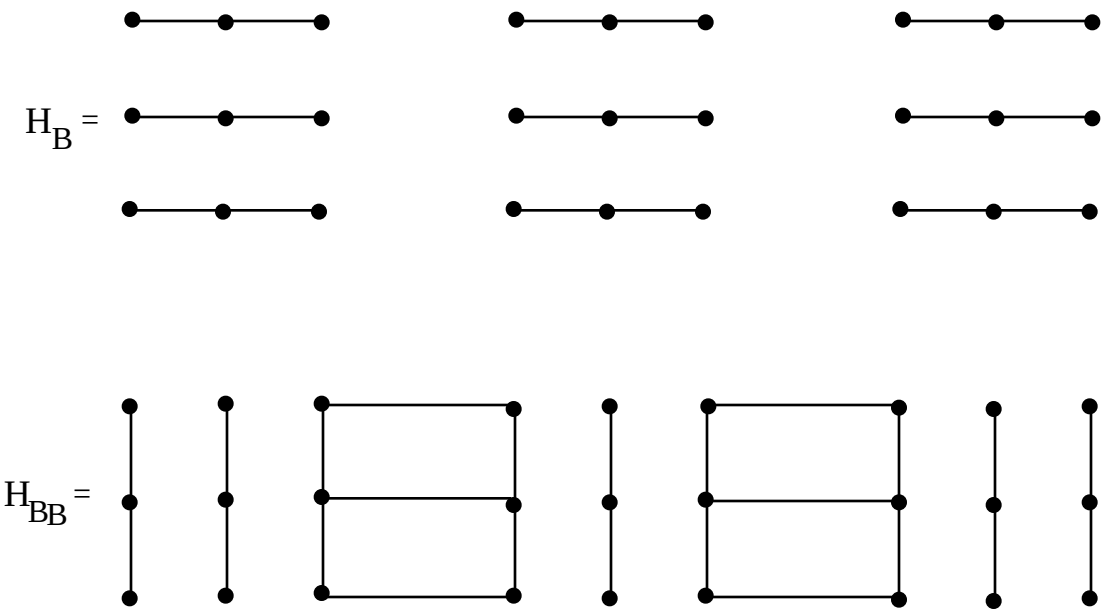

Figure 7